

## Detection of change in the Arctic using satellite and in situ data

Josefino C. Comiso

Laboratory for Hydrospheric Processes, NASA Goddard Space Flight Center, Greenbelt, Maryland, USA

Jiayan Yang, Susumo Honjo, and Richard A. Krishfield

Woods Hole Oceanographic Institution, Woods Hole, Massachusetts, USA

Received 14 February 2002; revised 18 December 2002; accepted 10 September 2003; published 24 December 2003.

[1] The decade of the 1990s was the warmest decade of the last century, while the year 1998 was the warmest year ever observed by modern techniques, with 9 out of 12 months of the year being the warmest months. Satellite ice cover and surface temperature data, European Centre for Medium-Range Weather Forecasts (wind), and ocean hydrographic data are examined to gain insights into this warming phenomenon. Areas of ice-free water in both western and eastern regions of the Arctic are found to have followed a cyclical pattern with approximately decadal period but with a lag of about 3 years between the eastern and western regions. The pattern was interrupted by unusually large anomalies in 1993 and 1998 in the western region and in 1995 in the eastern region. The area of open water in 1998 was the largest ever observed in the western region and occurred concurrently with large surface temperature anomalies in the area and adjacent regions. This also occurred at a time when the atmospheric circulation changed from predominantly cyclonic in 1996 to anticyclonic in 1997 and 1998. Detailed hydrographic measurements over the same general area in April 1996 and April 1997 indicate a warming and significant freshening in the top layer of the ocean, suggesting increases in ice melt and/or river runoff. Continuous ocean temperature and salinity data from ocean buoys at depths of 8, 45, and 75 m confirm these results and show large interannual changes during the 1996–1998 period. Surface temperature data show a general warming in the region that is highly correlated with observed decline in summer sea ice, while hydrographic data suggest that in 1997 and 1998, the upper part of the ocean was unusually fresh and warm compared to available data between 1956 and 1996. *INDEX TERMS*: 4215 Oceanography: General: Climate and interannual variability (3309); 1610 Global Change: Atmosphere (0315, 0325); 3349 Meteorology and Atmospheric Dynamics: Polar meteorology; 4540 Oceanography: Physical: Ice mechanics and air/sea/ice exchange processes; 4207 Oceanography: General: Arctic and Antarctic oceanography; *KEYWORDS*: Arctic Sea ice, climate change, surface temperature, wind, buoy, hydrography

**Citation:** Comiso, J. C., J. Yang, S. Honjo, and R. A. Krishfield, Detection of change in the Arctic using satellite and in situ data, *J. Geophys. Res.*, 108(C12), 3384, doi:10.1029/2002JC001347, 2003.

### 1. Introduction

[2] One of the key issues associated with climate change is the role of the Arctic in a warming scenario. Studies based on meteorological station data have indicated that global temperatures have been increasing at the rate of about 0.5°C per century with increases at a relatively high rate in recent years [Jones *et al.*, 1999]. The Arctic Sea ice cover, as inferred from satellite data from 1978 to 1996, has also been reported to be on the decline at a rate of about 3% per decade in extent [Bjorgo *et al.*, 1997; Parkinson *et al.*, 1999], while submarine studies have indicated a warming ocean and a thinning ice cover [Morison *et al.*, 1998; Rothrock *et al.*, 1999; Wadhams and Davis, 2000]. Further-

more, the ice sheet has been observed to be thinning around the periphery of Greenland [Krabill *et al.*, 1999], while glaciers in the Northern Hemisphere have been retreating [Burroughs, 1999]. And most recently, the perennial ice cover in the Arctic has been reported to be declining at the rate of 9% per decade [Comiso, 2002].

[3] Because of feedback effects associated with the high albedo of ice and snow, compared to that of open ocean, climate signals are expected to be amplified in the Arctic [Budyko, 1966; Manabe *et al.*, 1992]. However, the energy exchanges between the ocean, ice, and atmosphere in the Arctic are poorly understood because of limited surface measurements due to the general inaccessibility of the region. The magnitude and impact of these exchanges, at least in the central Arctic region, were previously believed to be minor compared to those that occur near the marginal ice zones. This is mainly because limited data have shown

that the Arctic Ocean is strongly stratified. This stratification is in part responsible for the scarcity of convection in the region and the maintenance of the thick perennial sea ice cover [Aagaard and Carmack, 1994]. However, the stratification is not uniform everywhere and large differences have been cited between the Canadian (western Arctic) Basin and the Eurasian (eastern Arctic) Basin, with the latter having much weaker stratification. Recent studies also indicate that while the marginal ice zones are indeed regions of intense activities, the inner zones covered mainly by consolidated ice are also sites of significant oceanographic, atmospheric, and biological activities [Aagaard et al., 1996; Carmack et al., 1995; Morison et al., 1998]. Moreover, the occurrence of storms in the region has been noted as causing considerable changes in the vertical structure of the upper part of the ocean [Yang et al., 2001].

[4] In this paper, satellite data are analyzed in conjunction with atmospheric, buoy, and other data to gain insights into the synergy between the geophysical variables and better understand the apparently changing state of the Arctic, especially the Arctic Ocean and its sea ice cover. The entire Arctic region is studied using about 20 years of sea ice and surface temperature data from satellite passive microwave and infrared data, respectively, and atmospheric data from the European Centre for Medium-Range Weather Forecasts (ECMWF) program. Both western and eastern regions are also studied separately, with more detailed studies done in the western region, where the primary buoys are located and where large anomalies were observed in recent years. The strategy is to quantify concurrent changes in ice concentration, surface temperature, sea level pressure, and ocean parameters and assess the relative sensitivity of these variables to a changing Arctic climate system.

## 2. Satellite and Buoy Observations

### 2.1. Multisensor Satellite Data

[5] Satellite data have previously been used in many Arctic Sea ice cover investigations [Gloersen et al., 1992; Kwok et al., 1996; Parkinson et al., 1999]. In this study, we use primarily passive microwave and infrared data because they are the only satellite data available with long enough record length to provide meaningful interannual variability and trend studies. Satellite passive microwave data provide synoptic coverage of the Arctic surface under day/night and practically all weather conditions. Multi-channel brightness temperature data from the Nimbus-7 scanning multichannel microwave radiometer (SMMR) and DMSP Special Sensor Microwave Imager (SSM/I) have been gridded to a polar stereographic format with a resolution of 25 km by the National Snow and Ice Data Center (NSIDC). These data are in turn converted to ice concentration maps, using the Bootstrap sea ice algorithm [Comiso et al., 1997] to generate a consistently derived history of the sea ice cover distributions from October 1978 to the present. The satellite swath width is about 1600 km, and the orbital period is about 110 min to enable revisits at most areas in the polar region, of as often as 6 times each day. However, only daily-averaged data have been archived, and this study uses mainly monthly and yearly averages derived from the daily data.

[6] Radiance data from the NOAA advanced very high resolution radiometer (AVHRR) are the primary source of satellite surface temperature and visible data. At a resolution of 1 km, this sensor provides spatial details that are not possible to obtain from the SSM/I sensor. In this study, we used global area coverage (GAC) data, which have been subsampled at a coarser resolution (4–6 km) but is the only long-term and continuous AVHRR data set available. The primary parameter derived from the GAC data is monthly surface temperature, derived using techniques discussed by Steffen et al. [1993] and Comiso [2000]. Surface temperature data can be derived only during cloud-free conditions. For convenience in the comparative analysis, GAC data have been mapped to a polar stereographic grid similar to that used for the SSM/I data but with a resolution of 6.25 km by 6.25 km, as described by Comiso [2000].

[7] Validations of our interpretation of passive microwave and infrared data have been done through the use of high-resolution satellite and aircraft data, including the synthetic aperture radar (SAR) and Landsat data [e.g., Kwok et al., 1996; Comiso et al., 1997], as well as ship and station data. SAR and Landsat provide complementary information in that SAR operates at a long wavelength and provides surface and subsurface information while Landsat, which is a visible sensor, provides surface information. The retrieved ice concentration products from passive microwave have errors of about 5–15%, depending on surface condition and season [Comiso et al., 1997], while the surface ice temperatures derived from AVHRR have errors estimated at generally about 2–3 K in the Antarctic [Comiso, 2000]. Comparative studies of AVHRR data with newly available and highly accurate in situ data from Surface Heat Budget of the Arctic Ocean (SHEBA) [Perovich et al., 1997] and the Greenland Project [Steffen and Box, 2001] yielded good agreement, with a standard deviation of 1.6 K and correlation coefficients of 0.98, indicating that the accuracy of the Arctic AVHRR data may be even better than previously reported.

### 2.2. Surface and Subsurface Buoy Data

[8] A complete description of the Ice-Ocean Environmental Buoy (IOEB) Program and the capabilities of the system are given by Honjo et al. [1995] and Krishfield et al. [1999]. The buoy provides a stable platform from which a consistent and reliable time series of atmospheric, ice, and ocean data can be obtained at its location. The data set is unique in that the buoys provide continuous monitoring of these variables, while satellite sensors provide near-simultaneous observations of surface parameters that might influence the ocean and ice conditions that are observed from the buoy system. Among the buoy data of interest are atmospheric variables such as air temperatures, wind, and humidity, ice variables such as snow and ice temperatures, and ocean variables such as temperatures, conductivity, and sigma  $t$ . The acoustic Doppler current profiler (ADCP) vectors also provide information about the direction of currents at different depths.

[9] The trajectories of the two buoys used primarily for this study together with the bathymetry of the Arctic are shown in Figure 1a. One of them, which we call IOEB, was installed on a 4-m ice floe on 26 April 1992 at 79.12°N and 132.22°W, but due to instrumental malfunction, the buoy

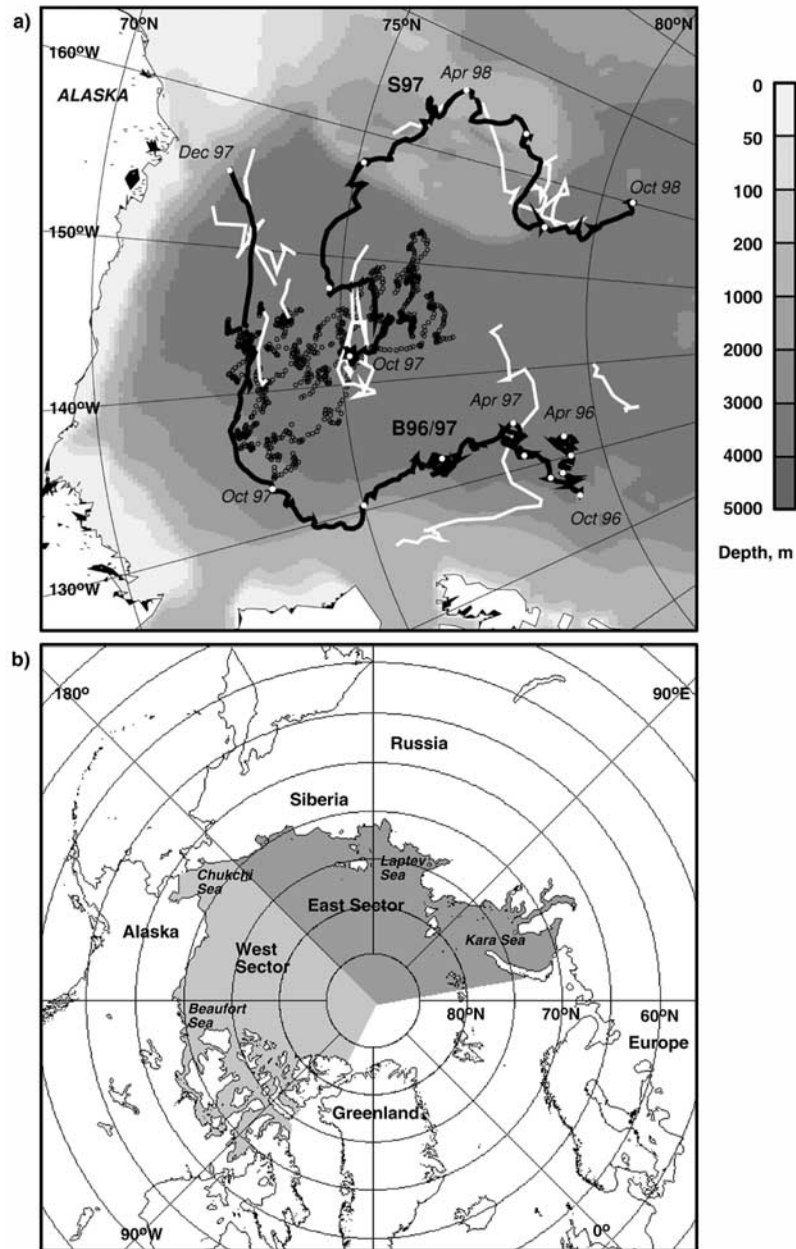


**Figure 1.** (a) Drift tracks of IOEB (April 1996 to December 1998 and labeled B96/97) and SHEBA IOEB (October 1997 to October 1998 and labeled S97) buoys in the Arctic. The bathymetry of the region is shown as different gray levels. Along the buoy track the white dots correspond to the location of the buoy on an every-other-month basis starting with April 1996 for B96/97 and October 1997 for S97. The white lines correspond to SALARGOS buoy tracks, while the small black circles correspond to the AIDJEX tracks. (b) Location map of the Arctic and the areal coverage of the western and eastern sectors (in different gray levels).

did not provide good ocean data until 27 April 1996, when it was refurbished. The same buoy was refurbished again on 11 April 1997, with slight modification on the ocean sensor system. The other buoy, called SHEBA IOEB, was installed on 30 September 1997 at 75.08°N, 140.92°W and collected continuous data up to October 1998. The locations of the buoy on an every-other-month basis are identified by white dots along the buoy tracks in Figure 1a.

[10] Temperature and conductivity water measurements were acquired by IOEB at depths of 8, 43, and 75 m from

April 1996 to April 1997, and at 8, 45, and 76 m from April 1997 to January 1998. Hereafter, the three depths will be referred to as 8, 45, and 75 m. Data were acquired internally on an hourly basis, but after April 1997 only telemetered data were available at a frequency of 6.5 per day. The SHEBA IOEB buoy provided observations at depths of 65, 105, and 165 m from October 1997 to October 1998. While not identical in depth coverage as the other buoys, values at about 65 m are expected to be coherent with those at 75 m and should provide useful

information about changes in the upper part of the ocean in 1998.

[11] Temperature and salinity calibrations were performed by the manufacturer of the instrument (SeaBird SeaCat) before and after each deployment. The accuracy of the temperature and salinity measurements has been estimated at about  $\pm 0.01^\circ\text{C}$  and  $\pm 0.05$  practical salinity unit (psu), respectively. Also, in the worst case scenario, the drift of the temperature sensor was less than  $0.004^\circ\text{C}/\text{yr}$  while that of the salinity sensor was less than  $0.02$  psu/yr. The computation of salinity from conductivity depends on depth. However, no correction to the salinity is applied since such adjustment is generally small in the depths considered. Also, the depth uncertainty due to the mooring tilt adds negligible salinity error in typical conditions and less than  $0.005$  psu at large speed. In addition to the IOEB time series data, conductivity-temperature-depth (CTD) profiles were obtained during buoy deployment operations in April 1996 (150-m depth) and April 1997 (500-m depth) using a Sea-Bird SBE-16 profiler. The precision of these profiles is better than  $0.005^\circ\text{C}$  and  $0.01$  psu for the temperature and salinity measurements, respectively.

### 3. Seasonal and Interannual Variability in the Sea Ice Cover and Open Water Area

[12] The Arctic sea ice cover goes through large seasonal and interannual variations, but changes were especially unusual in the Beaufort Sea from 1996 to 1998. A location map of the Arctic is shown in Figure 1b, which is oriented the same way as the buoy and satellite maps. To illustrate the magnitude of interannual variability from 1996 to 1998, color-coded ice concentration maps for these years at approximately the median date of freeze-up (i.e., on 12 October) are presented in Figure 2. The 1996 image represents the typical state of the Arctic ice cover during this period as observed from satellite data since 1973 [Gloersen et al., 1992; Parkinson et al., 1999]. The areal extent of the open water region in the Chukchi Sea/Beaufort Sea region was about  $3.0 \times 10^5$  km<sup>2</sup> in 1996, more than twice as much at  $7.0 \times 10^5$  km<sup>2</sup> in 1997, and about  $9.7 \times 10^5$  km<sup>2</sup> in 1998. Such dramatic changes in open water area are remarkable for a number of reasons. First, the open water area is in a region that is usually covered by thick multiyear ice. A replacement of multiyear ice by the seasonal first-year ice would make the average thickness of ice in the region substantially less in 1998 and 1997 than in 1996. Moreover, the predominance of first-year ice makes the region vulnerable to total melt and therefore the formation of open water in the subsequent summer. Second, a much larger open water area than average (as in 1998) allows for the absorption of larger amount of solar energy than normal and would cause increases in the temperature of the upper ocean layer [Maykut and McPhee, 1995]. Such increase in temperature could in turn inhibit the growth of ice in autumn and winter and accelerate the decay of ice in spring and summer, assuming that this heat is not lost due to storms or other factors. The process could cause a positive feedback that would lead to thinning in the ice cover. If this process continues, it would cause a gradual disappearance of the Arctic multiyear ice cover and profound changes in the Arctic Ocean and its environment.

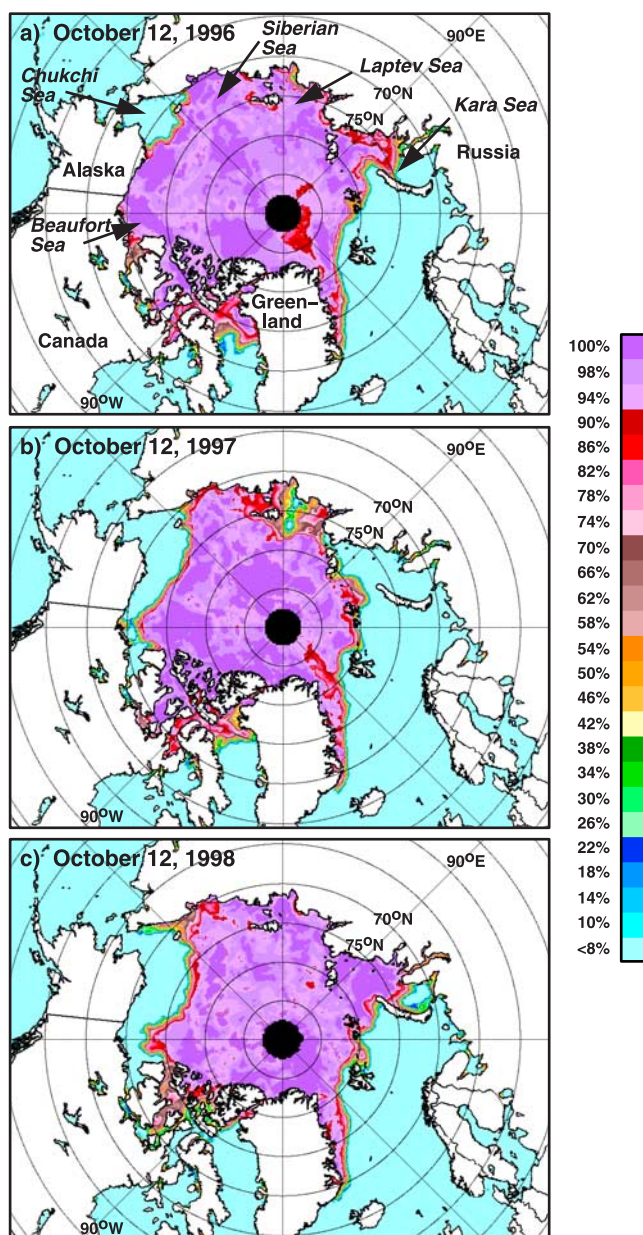


**Figure 2.** Color-coded ice concentration maps of the Arctic during the approximate mean period of autumn freeze-up on (a) 12 October 1996, (b) 12 October 1997, and (c) 12 October 1998.

[13] However, we already know that the open water area in the region in 1999 is not any larger than that of 1998. We also know that 1999 is not as warm a year as 1998 (P. D. Jones, private communication, 2000). It is thus important to realize that effects of environmental factors in the region are not easy to interpret. It is known that the Arctic sea ice cover is influenced by periodic changes in atmospheric wind circulation as influenced by changes in wind patterns [Mysak, 1999]. The Arctic ice cover is not stationary but is very dynamic and undergoes changes in ice drift patterns and wind circulation from the dominant anticyclonic (clockwise) circulation of the Arctic gyre to a cyclonic (counterclockwise) circulation [Proshutinsky and Johnson, 1997].

## September Ice Concentration Anomalies

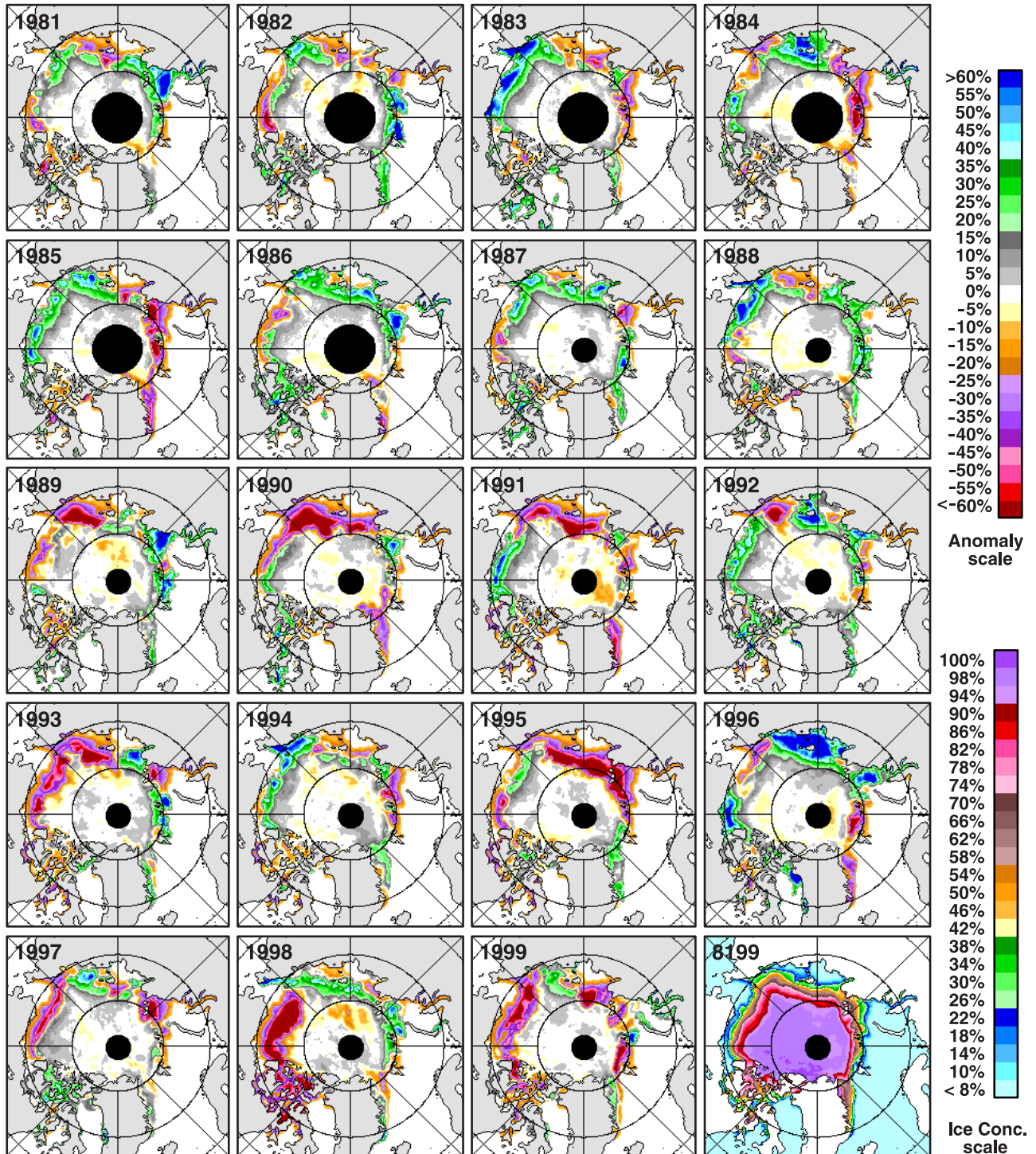


**Figure 3.** Color-coded monthly anomalies in ice concentration for each September (during ice minima) from 1981 to 1999. The last image labeled 81–99 is the average of all the September ice concentrations from 1981 to 1999. Each anomaly map was derived by taking the difference of the monthly average ice concentration and the 81–99 average.

Thus a large change in open water area in the Beaufort Sea over a 3-year period does not necessarily reflect a long-term change in the ice patterns.

[14] To illustrate the changing behavior of the Arctic Sea ice cover on a longer-term basis, monthly ice concentration

anomaly maps during each September (i.e., at ice extent minimum) from 1981 to 1999 are shown in Figure 3. The color-coded images show where the average ice concentrations are anomalously low (reddish color) and where they are anomalously high (bluish) in any one year. Areas where

ice concentrations are anomalously very low (dark red) are normally areas of open water during the summer. Changes in areal coverage of the red (and purple) pixels from 1 year to another thus represent how open water area changes on a year-to-year basis. For reference, the climatological ice concentration data (average of ice concentration data from 1981 to 1999) used in the calculation of the anomalies for each year are shown in the last image of Figure 3. The ice cover during summer minima represents the state of the perennial sea ice cover, which consists mainly of thick multiyear ice. The average thickness of the perennial ice is about 3 m, but in heavily deformed areas, the ice can be as thick as 10–20 m over 50-km segments north of Greenland [Wadhams, 1988]. The blue (and green) pixels are usually areas of anomalously high concentration and where much of the multiyear ice in the peripheral regions are advected. During some years, perennial sea ice covers much of the Beaufort Sea (e.g., 1983, 1985, 1988, 1991, 1992, 1994, and 1996) while in other years, large open water areas in the region are apparent, including 1990, 1993, 1997, 1998, and 1999. The spatial extent of the anomalies is fully depicted for each year, and it is interesting to note that most of the big negative anomalies (reds) occurred in the 1990s. Note also that during the satellite era, 1997–1999 was the only time that open water was large in the Beaufort Sea region for three consecutive years.

[15] Quantitatively, the extent and actual areas of the ice cover in the Arctic have been declining, as reported previously [Bjorgo *et al.*, 1997; Parkinson *et al.*, 1999] using 1978–1996 data. An updated version of the trend analysis using the November 1978 through December 2000 data is shown in Figure 4, and the results are generally consistent with previous reports. The ice concentration maps used in this study were derived using the Bootstrap Algorithm as described by Comiso *et al.* [1997]. Monthly ice extent and ice area anomaly distributions are shown in Figures 4a and 4b, and the trends in the data are shown to be  $-2.0 \pm 0.3\%$  per decade and  $-3.1 \pm 0.3\%$  per decade, respectively. The difference in trend values between ice extent and ice area is mainly due to the negative trend in ice concentration during the same period (Figure 4c). Low values in average ice concentration during the summer period are evident in 1989, 1993, 1995, 1998, and 1999. This can be due in part to possible increases in the areal extent of meltponding (due to warming), which can cause a slight negative bias in the microwave data [Comiso and Kwok, 1996], but analysis of the same data set that excludes the summer data yielded similar trends. The ice extent and ice area were low during these years and also in 1990 and 1991. The predominance in the number of low values in the 1990s compared to the 1980s is consistent with a declining sea ice cover, as the negative trend results indicate.

[16] As the ice melts and the ice cover retreats from the land/ocean boundary during the summer, a significant fraction (about 30%) of the Arctic Ocean area becomes ice free, as indicated previously, and is directly exposed to the atmosphere. The areal extent of the open water and how it changes with time is of interest because of its impact on the heat budget and mass balance of ice in the region. To quantify temporal changes in the open water extent, it is convenient to divide the Arctic region into eastern and western sectors, as indicated in Figure 1b. The western

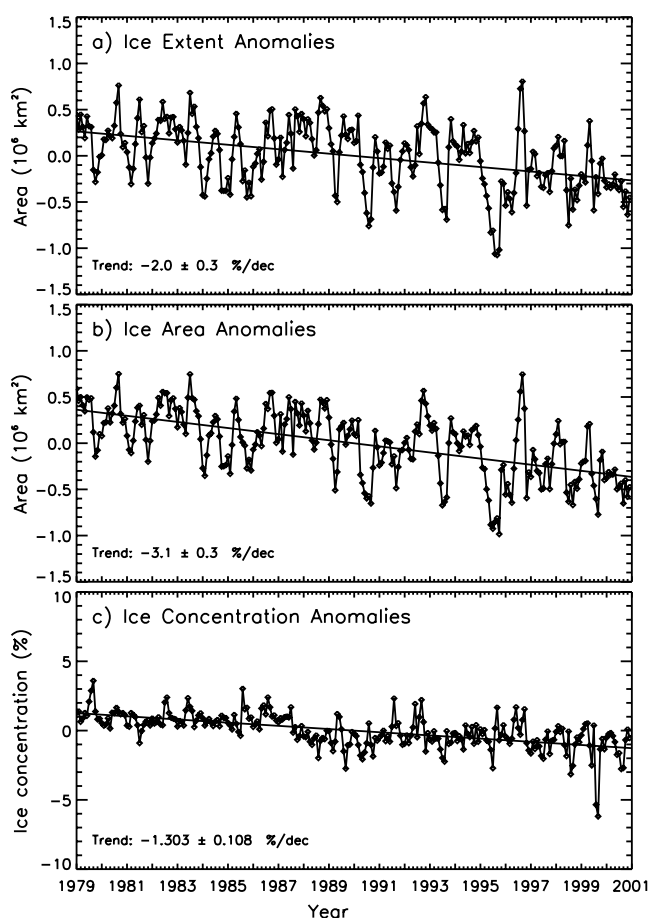


**Figure 4.** Plots of anomalies in monthly (a) ice extent, (b) actual ice area, and (c) ice concentration and the results of trend analysis for the period from 1979 to 2000. The trend results are expressed in percentage per decade. See text for trends in units of area.

sector includes data from the Chukchi Sea, the Beaufort Sea, and the Canadian Archipelago, while the eastern sector includes data from the Siberian, Laptev, and Kara Seas. The boundary of these two sectors was chosen in a semiarbitrary manner but is a good logical choice for separating the big anomalies in the western and eastern regions, as indicated in Figure 3. A third sector that covers the rest of the Arctic was not analyzed because of the complexity in the ice cover distribution (as well as environmental forcing) in the region.

[17] The monthly areal extent of open water derived from passive microwave ice concentration data from August 1981 to July 2000 in the western and eastern sectors are shown in Figures 5a and 5b, respectively. The plots show that the open water area goes through large seasonal and interannual variability. By inspection, the maximum value for each year (with the exception of the anomalously high values in 1993 and 1998 in the western sector and 1995 in the eastern sector) follows a sinusoidal pattern. The dotted lines are sinusoidal fits to these maximum values (anomalously high values excluded), and period of the cycle is estimated as approximately 10 years from this relatively short data set with the western sector, leading the eastern sector by about 3 years. This suggests the existence of a

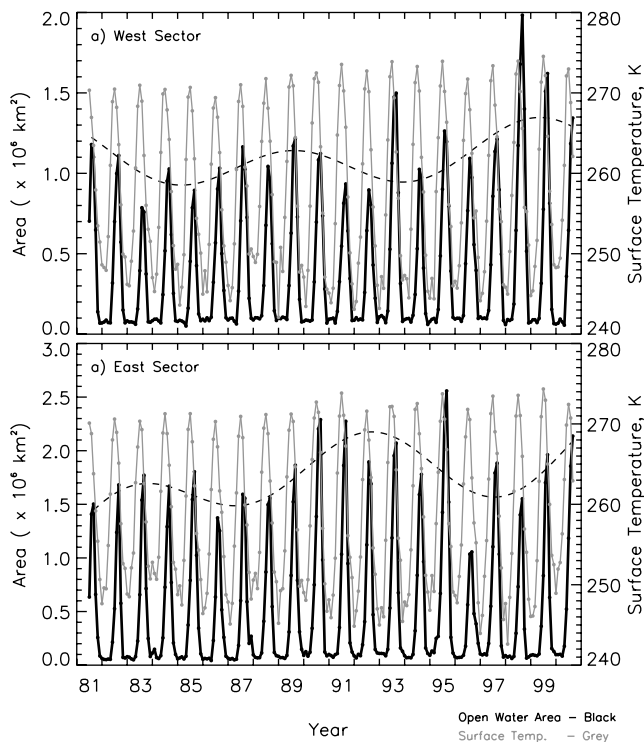


**Figure 5.** Estimates of open water area (black line) and average surface temperature (gray line) of the ice-covered area (where the ice concentration is  $>80\%$ ) from 1981 to 2000 in (a) the western sector and (b) the eastern sector. The dashed line is a sinusoidal fit to the maximum open water area, with the exception of 1993 and 1998 for the western sector and 1995 for the eastern sector.

decadal forcing mechanism that propagates around the Arctic. Plots of coincident surface temperatures derived from infrared satellite data are also shown by thin lines in Figure 5, and they generally show good coherence with the open water areas, as will be discussed in the next section.

[18] In the western sector, the maximum open water area, which occurs during late summer, fluctuates from about  $0.8 \times 10^6$  to about  $1.2 \times 10^6$  km<sup>2</sup>. The 20-year record shows low values in 1983 and 1992 and relatively high values in 1987, 1989, and 1995. In 1993, however, the extent was abnormally high at  $1.5 \times 10^6$  km<sup>2</sup> instead of a minimum value of about  $1.0 \times 10^6$  km<sup>2</sup>, as suggested by the dashed line for a normal cycle. In 1998, the value is even more abnormal at  $2.0 \times 10^6$  km<sup>2</sup>, compared to a near-peak dashed-line value of about  $1.3 \times 10^6$  km<sup>2</sup>. This is the largest open water area in the western region during the satellite era. It is apparent that the anomalies are not caused by the same forcing that drives the cyclical pattern. Among the possible candidates is the big El Niño-Southern Oscillation (ENSO) event in 1998 and the relatively smaller one in 1993. To establish such a connection would require a separate study that is beyond the scope of this paper.

[19] In the eastern sector, a periodic pattern in the maximum extents of open water is also apparent, with the maximum in the 1980s significantly lower than those in the 1990s, suggesting more ice melt occurring in the latter decade. In the 1980s the values range from  $1.4 \times 10^6$  to

$1.8 \times 10^6$  km<sup>2</sup>, while in the 1990s the normal range is from  $1.1 \times 10^6$  to  $2.3 \times 10^6$  km<sup>2</sup>, with dips in 1986 and 1996. Following the pattern suggested by the dashed line, 1995 was supposed to be a year in which the summer open water area is low, but it was instead a year when a record open water area in the region ( $2.6 \times 10^6$  km<sup>2</sup>) was observed. Figure 4 also shows that the lowest extent of ice in the Arctic recorded by satellite data occurred in 1995. Modeling results [Zhang *et al.*, 2000] show that during the period of high NAO from 1989 to 1996 there was a substantial reduction of ice advection into the eastern Arctic from the Canadian Basin and an increase in ice export through Fram Strait. Figure 5b indicates enhanced open water area during this period, except in 1992 and 1996. The changes from the 1980s to the 1990s may also be associated with the trend in the Arctic Oscillation (AO) toward a high index polarity, as reported by Rigor *et al.* [2002]. However, the correlation of summer maximum values of the open water with AO indices is rather low, with the correlation coefficient being about 0.2. A more detailed analysis of the relationship of the ice cover with AO is not within the scope of this paper.

#### 4. Seasonal and Interannual Variability in Surface Temperature

[20] Satellite thermal infrared data currently provide the only synoptic and continuous observation of surface temperatures in polar regions [Comiso, 2000]. Using Arctic surface temperature AVHRR data described by Comiso [2001], anomalies in monthly temperatures for each September from 1981 through 1999 are presented in Figure 6. The last image in Figure 6 is the average of the September temperatures from 1981 to 1999, which was used as the climatology for estimating monthly anomalies. These anomaly images are especially useful because they provide data not only over sea ice but also over adjacent land and open ocean. Unusually warm areas are indicated by warm (yellow, red, and purple) colors, while unusually cold areas are represented by cold (gray, green, and blue) colors. The maps indicate a predominance of anomalously warm temperatures during the 1990–1999 period, especially in locations where there were large open water areas during the summer. The slight cooling events in 1992 and 1993 may be partly due to the Mount Pinatubo volcanic eruption in 1991. In most cases, anomalously warm areas extend into the land and open water areas, indicating that atmospheric warming is at least in part responsible in the observed retreat of the Arctic Sea ice cover. This is also a manifestation that a third influence, i.e., atmospheric circulation anomaly, may be responsible in the ice and temperature anomalies.

[21] Anomalies on a month-to-month basis from June to October (except the Septembers which are already presented in Figure 6) during the 1996–1998 period are shown in Figures 7. The images indicate that the temperature anomalies are not just a late summer phenomenon and that changes are also apparent during other periods. The data indicate that June 1996 was a relatively cold month in the Arctic compared to June 1997 and June 1998. The positive anomalies are also higher in the central Arctic, Beaufort Sea, and North America in 1998 than in 1997. July 1996 was again a relatively cold month in the central Arctic

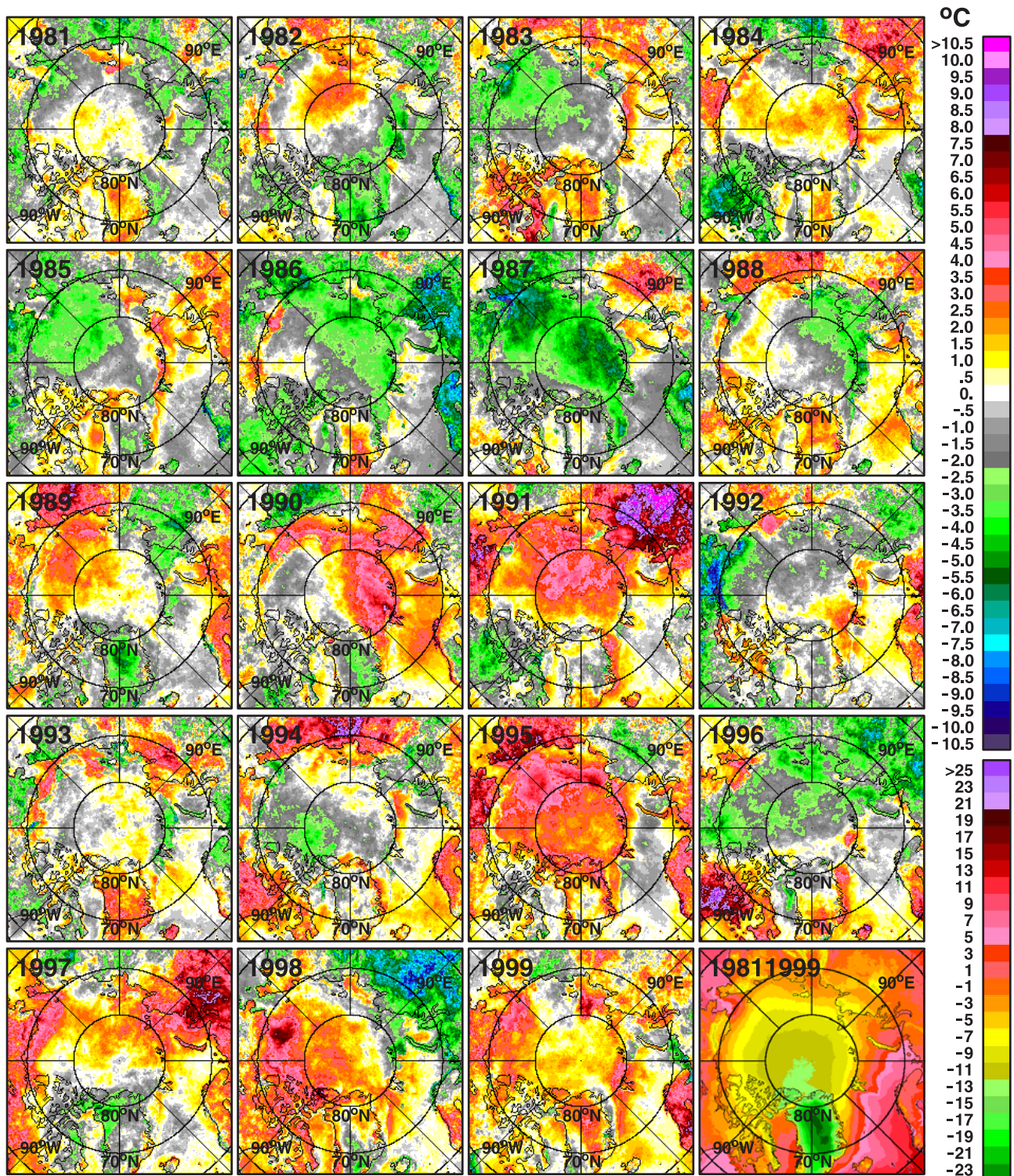


**Figure 6.** September surface temperatures anomalies from 1981 to 1999. The last image labeled 81–99 corresponds to the average of all September temperatures from 1981 to 1999. Each anomaly map was derived taking the difference of the September average and the 81–99 average.

compared with July 1997 and July 1998. In August, the data show even more negative anomalies than in the previous months of 1996, while the anomalies are generally positive in August 1997 and 1998, with a significant warming in Eurasia in August 1997 and a cooling in the same region in August 1998. In October, there was a general cooling

in 1996 and 1997 but a warming in 1998 in North America. Meanwhile, the warming in Eurasia in September 1997 continued on through October 1997 while the cooling in the same region in September 1998 continued on through October. It should be pointed out that except for Alaska, it was also anomalously warm from June through Septem-

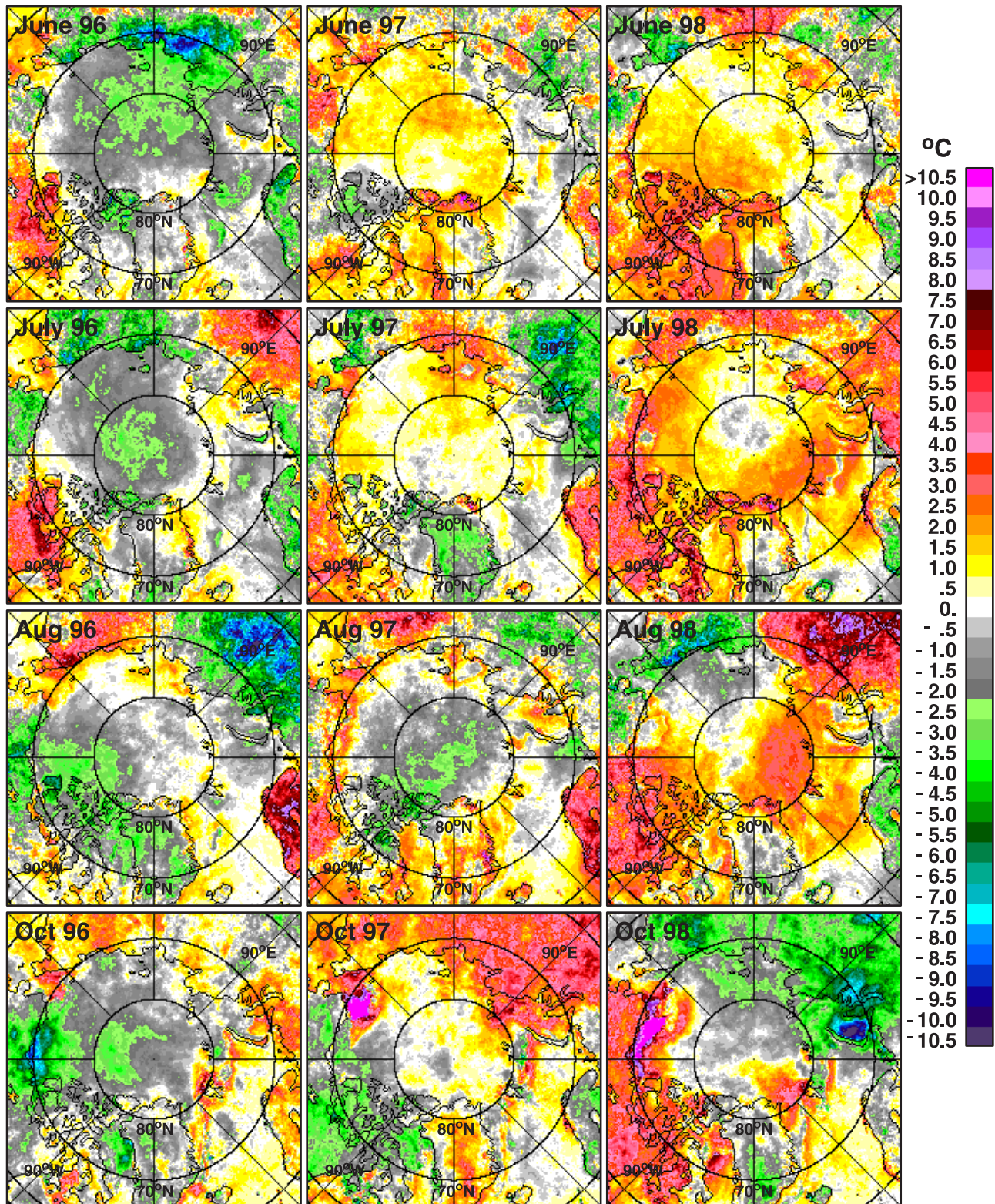


**Figure 7.** Color-coded monthly anomalies in surface temperatures in June, July, August, and October of 1996, 1997, and 1998 using AVHRR data. Anomalies were calculated using the climatology data from 1981 to 1999.

ber in North America in 1996. The negative anomalies in Alaska and in the western Arctic Ocean in September–October of 1996 are consistent with early freeze-up and the relatively low open water in the region on 12 October

(Figure 2). Conversely, the persistently warm anomalies in the western Arctic from June to October in 1998 are consistent with the existence of large open water areas in the region during the summer and early autumn of 1998.

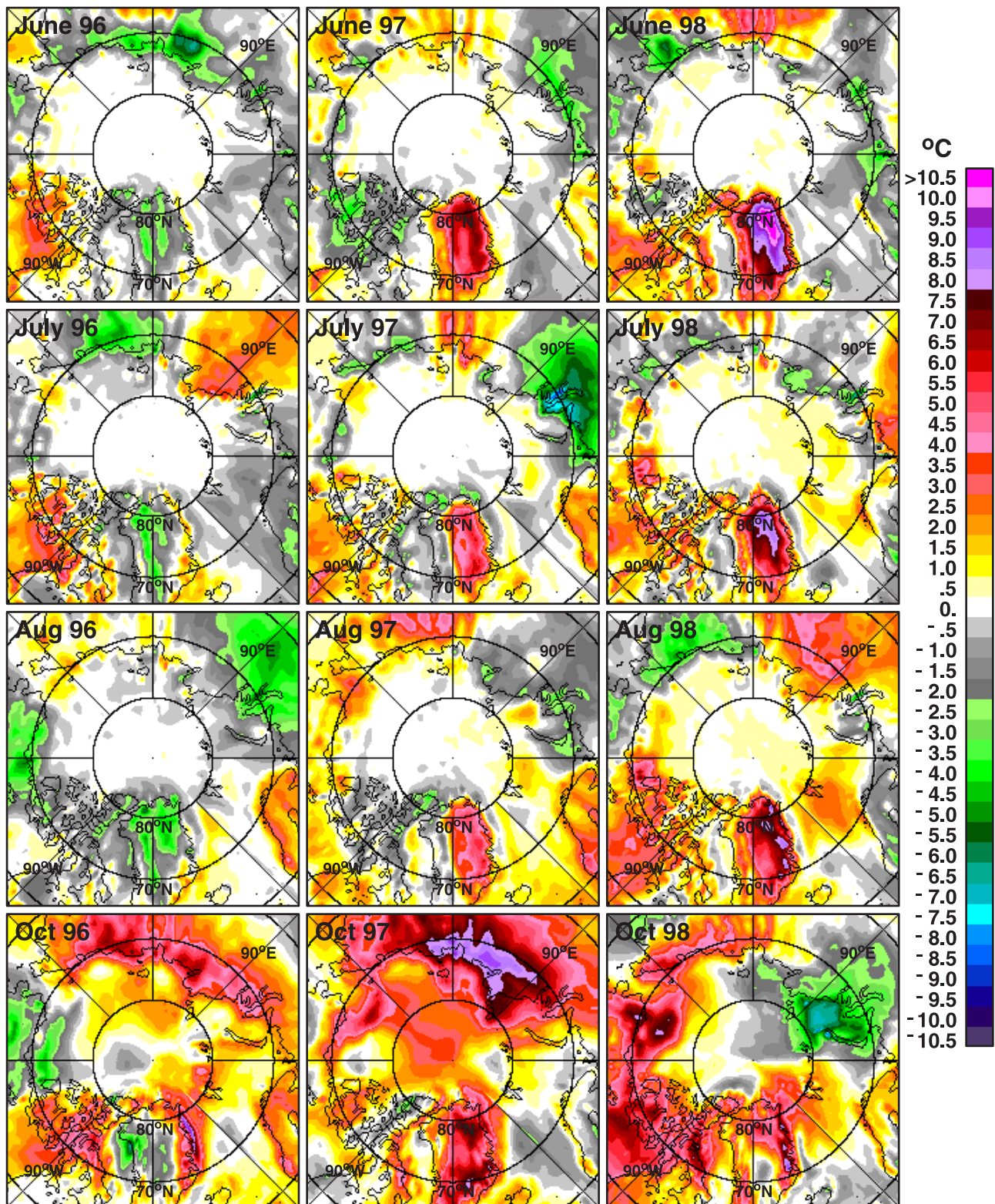


**Figure 8.** Color-coded monthly anomalies in surface temperatures in June, July, August, and October of 1996, 1997, and 1998 using ECMWF data. Anomalies were calculated using the climatology data from 1981 to 1999.

[22] Images similar to those of Figure 7 but using ECMWF surface temperature data are presented in Figure 8. While significant differences between the two data sets are apparent in the central Arctic, the patterns of positive and negative

anomalies around the periphery are very similar. For example, the location and extent of negative anomalies in the August 1996 image in Figure 7 is basically reproduced in Figure 8. The patterns of positive anomalies in August 1998 are also

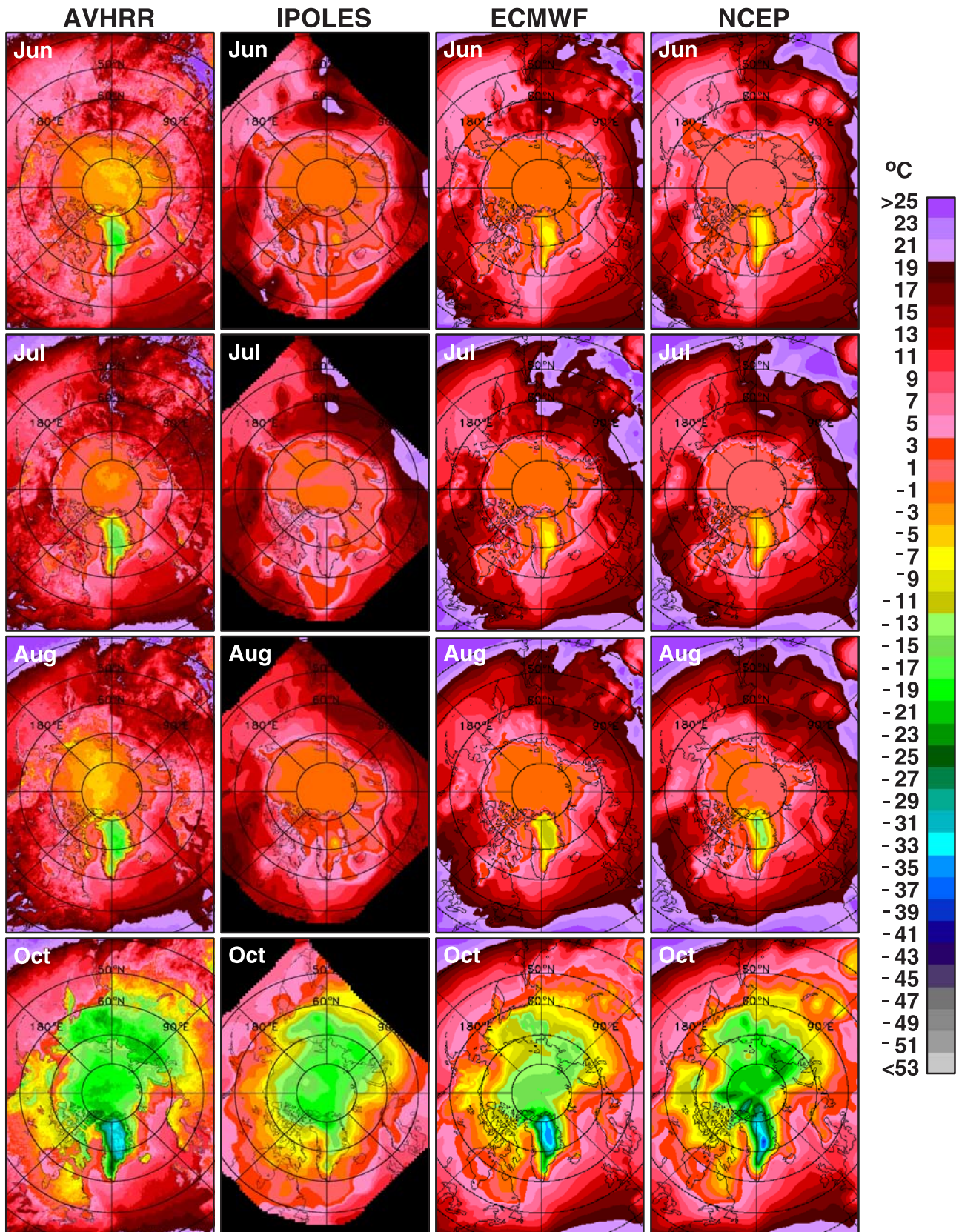


**Figure 9.** Color-coded monthly surface temperatures in June, July, August, and October 1998 using four different data sets: AVHRR, IPOLES (IABP/POLES), ECMWF, and NCEP.

very similar for the two data sets. In October 1998, negative anomalies in Siberia in the AVHRR data are shown as positive anomalies in the ECMWF data. However, other data sets (e.g., IABP/POLES as reported by *Rigor et al.* [2002]) show better consistency with the AVHRR data in this area. In general, however, it is apparent that the patterns of warming anomalies observed in the AVHRR data in the periphery of the central Arctic during the summers of 1996–1998 are also reflected in the ECMWF data set.

[23] In the central Arctic, the ECMWF data show practically no change in the central region during the summer months, while the patterns have some similarities with AVHRR data in October, especially in 1998. To gain insight into these discrepancies, actual monthly averages of surface temperatures using four different data sets are presented in Figure 9. In addition to AVHRR and ECMWF data, we show data from International Arctic Buoy Program/Polar Exchange at the Sea Surface (IABP/POLES) and National Centers for Environmental Prediction (NCEP) reanalysis obtained from National Center for Atmospheric Research (NCAR). It is apparent that the general patterns of high and low temperatures are very similar in the various images, but there are discrepancies in spatial distributions. The four data sets consistently show July as the warmest month, and the values also are generally consistent. However, for the other months, the values during the summer are significantly different, especially in the central Arctic. In these regions, there is practically no change in the central Arctic for ECMWF and NCEP data during summer months and little change for the POLES data. ECMWF data are, however, generally colder than NCEP data by about 2 K. The almost zero anomalies in the ECMWF data in Figure 8 in such large areas are thus caused by basically constant values throughout the summer months and for all years. Relatively constant temperatures in the region have been confirmed by some studies [*Lindsay, 1998*] for July but this is based on 2-m air temperatures, which may differ significantly from surface temperature at this time of the year. Also, the study is based on 50 years of historical Russian ice station data that are sparsely distributed and exclude the 1990s. The cause of the discrepancy with AVHRR is not known and can be partly due to persistent cloud cover during the summer and partly due to the shortcomings of the models. The results from all four, however, show very similar warming patterns and only the AVHRR data provide direct observations at all data points.

[24] Monthly averaged surface temperatures from AVHRR over sea ice-covered areas with concentrations greater than 80% are also plotted (gray line) in Figure 5. The plots show that the peak of the open ocean area distribution lags that of the surface ice temperature peak by about 2 months. The reason for this is that while peak temperatures are reached in July, the ice continues to melt until the temperature goes down below freezing temperatures in September. It is apparent that the open water areas in both western and eastern sectors are generally correlated with surface temperatures. For example, when the open water areas were high in 1993 and 1998 in the western sector, the average surface ice temperatures in the sector were also relatively high. Similarly, the high open water area in 1995 in the eastern sector occurred at the same time as when the average surface temperature was relatively high. It is logical to expect such a relationship since ice grows or decays, depending on

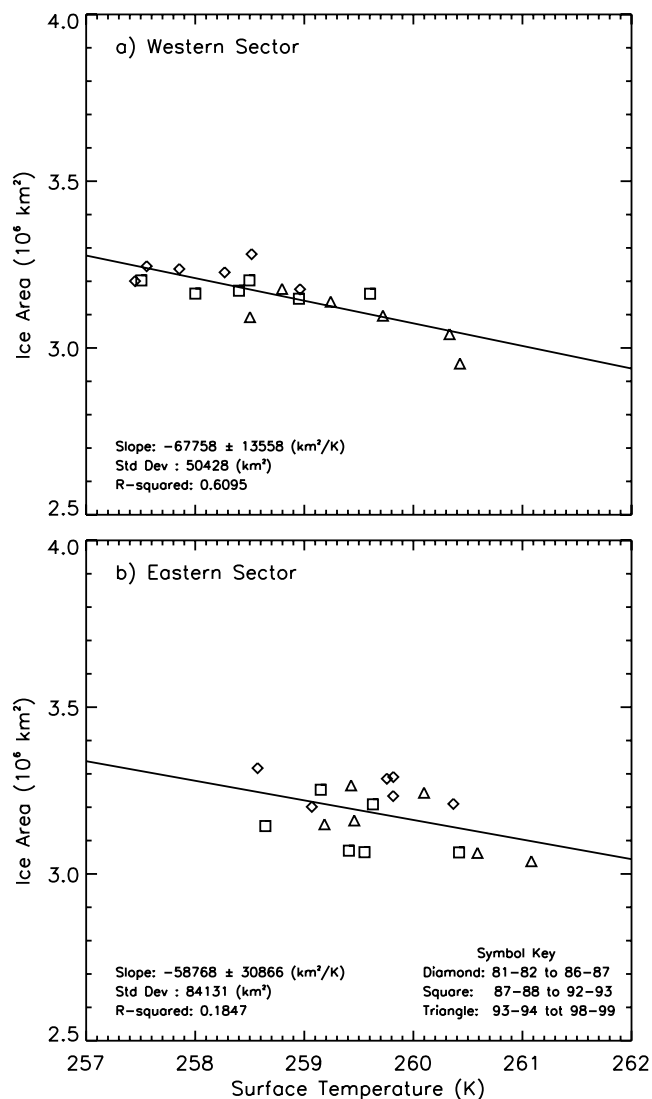


**Figure 10.** Sea ice area versus surface temperature using yearly average data from 1981 to 1999 and regression results. The yearly average is the average of monthly data from August of one year to July of the following year. The data points in diamonds, squares, and triangles are for different time periods, as indicated.

surface air temperature, but the strength of this relationship is not known because of complications associated with other factors. There are also exceptions, a good example of which is 1983 in the western sector.

[25] To quantify the strength of the relationship, the yearly average areas of the ice cover are compared with yearly average surface temperatures for the western sector and the eastern sector in Figures 10a and 10b, respectively. In the western sector, the correlation between the two variables is good, with the correlation coefficient being  $-0.61$ , while regression analysis shows that the ice area decreases by  $6.8 \pm 1.3 \times 10^4 \text{ km}^2$  per Kelvin increase in temperature. In the eastern sector, the correlation coefficient is only  $-0.18$ , while the regression result shows a decrease in the ice area of  $5.9 \pm 3.1 \times 10^4 \text{ km}^2$  per Kelvin increase in temperature. Ice-covered areas are shown to be better correlated with surface temperature in the western region

than in the eastern region. The reason is likely that of differences in the environment since the open water in the western region is confined and surrounded by land and sea ice while part of the eastern region is directly exposed to the Atlantic Ocean, the influence of which on the variability of the open water area is likely significant. Recent studies, however, reported that the average summer ice temperature is strongly correlated with the area of ice at the end of the summer, the correlation coefficient being  $-0.82$  [Comiso, 2002]. The correlation coefficients are not any higher because the influence on the ice cover of factors other than surface temperature can be considerable, as discussed in the following section.

## 5. Changes in Wind Patterns

[26] Strong persistent wind during the ice season can lead to a significant redistribution of the perennial ice cover consisting mainly of multiyear ice floes. Wind effects are important considerations in light of observed decreases in sea level pressure in the central Arctic [Walsh *et al.*, 1996]. The interannual effect of wind is clearly illustrated in Figure 1a, which shows that ice advection, represented by the buoy drift, was much more restricted in 1996 than in 1997 and 1998. Since the perennial ice cover is much thicker than the seasonal ice cover and more likely to survive the summer, the relative location of the perennial ice cover is important in terms of open ocean area distribution. Thus the open water area may be large at the Beaufort and Chukchi Seas during some years because the perennial ice cover is advected to the west (into the eastern sector), while it is not so large during other years because of the dominance of multiyear ice in the region. The same phenomenon applies to other regions like Laptev and Kara Seas. Strong winds also lead to considerable ridging and compaction that affect the thickness distribution (and drag coefficient) of the ice cover.

[27] To test whether this phenomenon applies to the variability of open water areas from 1996 to 1998, average ECMWF geostrophic winds during 4 months (June, July, September, and October) around summer and autumn are shown in Figure 11. ECMWF winds are used instead of ice drift data [e.g., Kwok *et al.*, 1998] because there are no data for the latter during the summer period (due to large uncertainties). However, comparative studies have shown good coherence of available ice drift data (including those from buoys) with ECMWF wind vectors. In Figure 11, monthly wind vectors are superimposed on color-coded monthly ice concentrations for the June-October period, except for August. Because of constantly changing wind values, monthly averages are used instead of hourly or daily values since the former makes it easier to assess the overall impact of wind during the different summers. It is apparent from the set of images that wind data indeed show interannual changes that may explain some of the observed spatial distribution of the ice cover. In 1996, the Arctic wind is predominantly cyclonic, with intensity and center location varying from 1 month to another. During the year, strong westerly wind is apparent along the Beaufort Sea in June, July, and August (not shown), changing to northerly in September and back again to westerly in October. In 1997, when there is more open water in the Beaufort Sea than in

1996, anticyclonic pattern is dominant in the Arctic Basin, with strong easterly wind in the Beaufort Sea especially in September. In 1998, the wind patterns are similar to those of 1997 but are more persistent in one direction and are relatively stronger. It is interesting to note that in July, similar cyclonic patterns are apparent for both 1996 and 1998 near the North Pole, but in the Beaufort Sea near the Alaska coastline the wind direction in one year was opposite that of the other year.

[28] Figure 11 suggests that the variability of sea ice concentration and open water area in the Beaufort Sea may have been influenced by the variability in the direction of surface wind. This is consistent with previous studies which have emphasized the role of wind-stress-driven variations. Sea ice in Arctic Ocean tends to drift in a direction roughly with an angle of  $5^{\circ}$ – $18^{\circ}$  to the right of the geostrophic wind [Thorndike and Colony, 1982] and with a somewhat smaller angle to the right of the surface wind at 10-m height. During periods when cyclonic wind dominates, as in the summer of 1996, sea ice is advected from the East Siberian Sea, Chukchi Sea, and the central Arctic toward Beaufort Sea, resulting in a buildup of multiyear ice in the western region. Meanwhile, the cyclonic wind can cause divergence of sea ice from the low mean sea level (msl) pressure center because the Coriolis force diverts ice to the right of the wind direction in the Northern Hemisphere. Such divergence of multiyear ice from the central Arctic toward the Canadian Basin would have contributed to the observed high sea ice concentration and reduced open water area in the Beaufort Sea in 1996. Alternatively, anticyclonic wind advects thick multiyear ice from the western region to the eastern region, and the divergence of sea ice from Canadian land-sea boundary toward the central Arctic Basin (due to Coriolis effect) would cause large open water areas to be formed in 1997 and 1998. It is likely that the open water area in the western section was larger in 1998 than in 1997 partly because the westerly wind was more persistent and generally stronger in 1998. The lower ice concentration in 1998 may also be due to the accumulative effect from 1997. After a large opening in the previous summer, the Beaufort Sea region was probably covered by thinner ice that is easier to melt completely before the summer of 1998.

[29] To study the interannual variability of wind direction and how consistently it affects the distribution of the sea ice cover during the summer, averages of wind vectors from January to July were calculated for each year from 1981 to 1999, and the results are presented in Figure 12. The average over 7 months is used to assess the overall impact of ice advection during the months immediately preceding the middle of summer. Vectors which are smaller than the size of the arrows ( $<0.5$  m/s) are not shown for clarity of presentation and since their net effect is relatively small. Also, ice drift is relatively slow, as illustrated in Figure 1a, and the typical advection rate is about 500 km (20 satellite pixels) in 7 months. The last image in Figure 12 is the average of all the 7-month vectors (1981–1999) and can be used as a reference in the interpretation of the vector maps for each year. The wind data are superimposed on the difference map of monthly ice concentrations between June and August for the same year to illustrate how the retreat of sea ice in the summer is influenced by such wind-driven ice advection. The set of images show large year-to-year

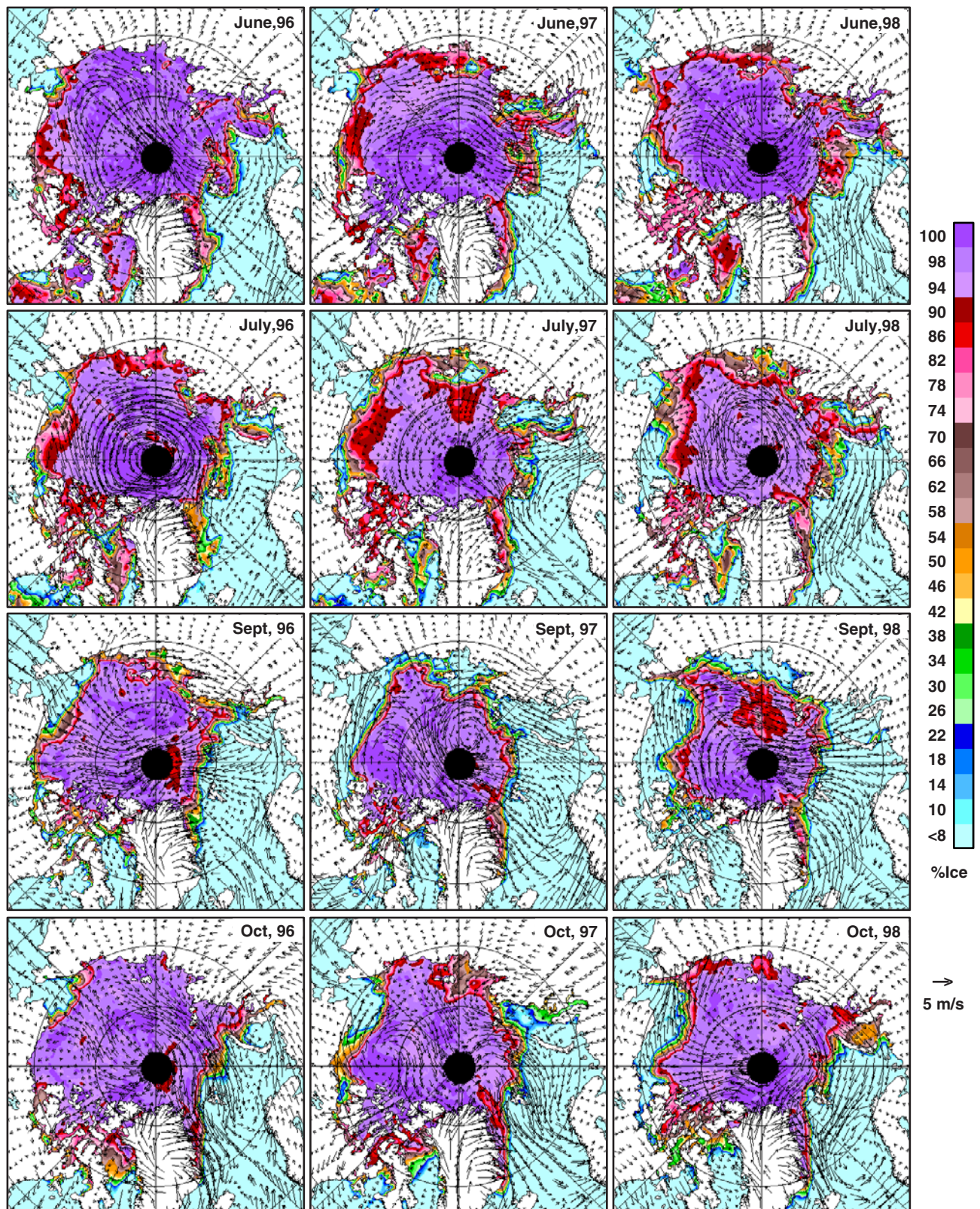


**Figure 11.** Monthly wind vectors (from ECMWF) over monthly ice concentration maps in June, July, September, and October of 1996, 1997, and 1998.

variability in the wind vectors. It is apparent that the vectors do not always exhibit either a cyclonic or anticyclonic pattern, making it difficult to infer the dominant atmospheric circulation for each year. This may be partly because

of the averaging over several months of data. The 7-month averages for 1996, 1997, and 1998 are, however, generally consistent with the more temporally detailed data in Figure 11. Inspection of the interannual variability of the

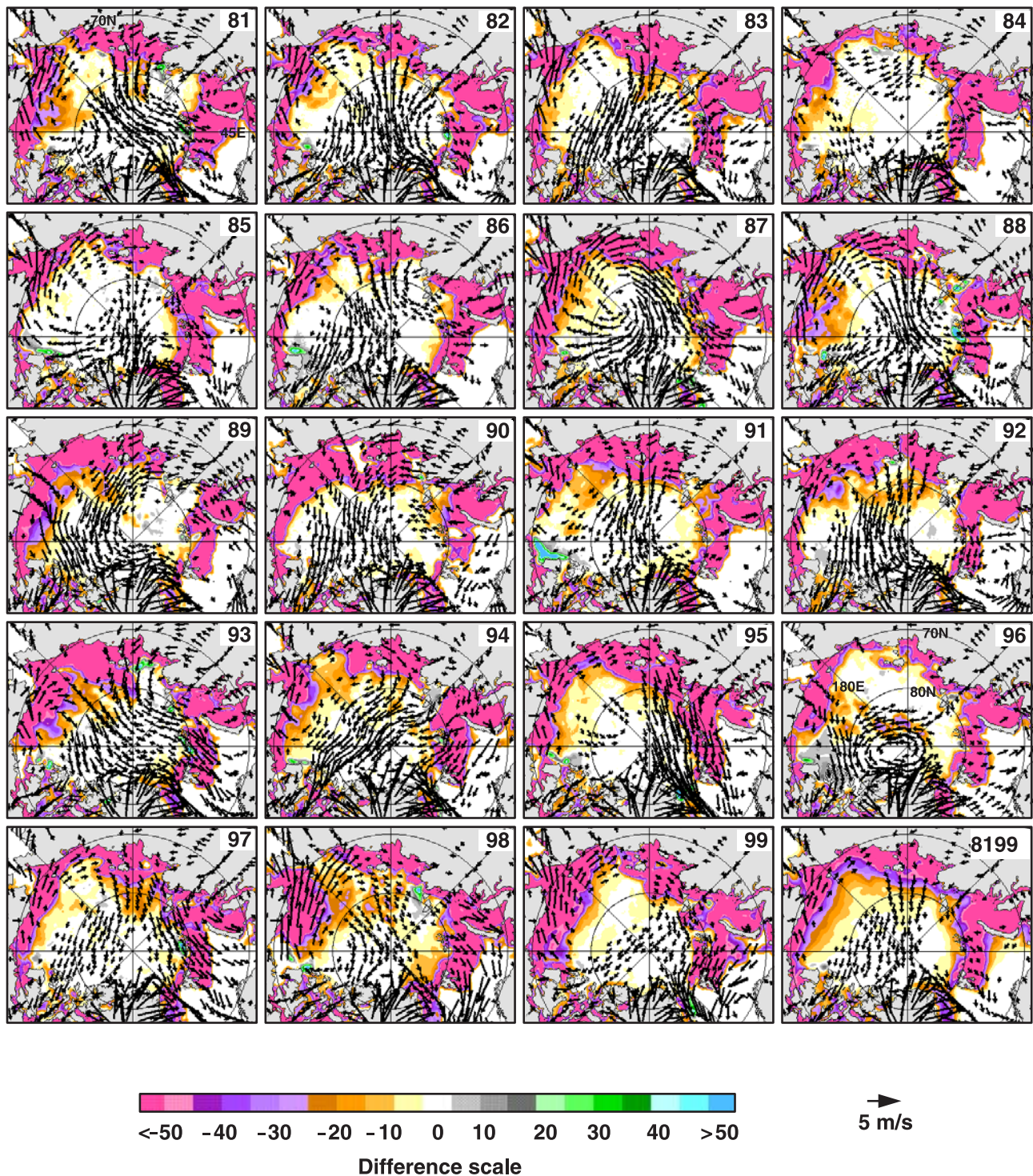


**Figure 12.** Wind vector averages (January–July) for each year from 1981 through 1999. The 7-month average provides the means to assess net effect of wind on the ice cover before the middle of summer. The last image is the overall average of the January–July vectors from 1981 through 1999. The background is the corresponding difference map of ice concentrations between June and August for each year.

vectors for some months (e.g., May, June, and July) also shows similar classification problems for the other years. Analysis of seasonal averages also yielded similar results.

[30] Generally, the wind vectors appear to be mainly in anticyclonic mode, as indicated by the 1981–1999 average,

but at different strength and coverage for the different years. A comparative analysis of the yearly patterns of the 7-month wind vectors with the corresponding ice concentration difference maps, as well as the September ice concentration anomalies (Figure 3), indicates that the area

of open water in the western region is not always influenced by atmospheric circulation, as revealed by the wind vectors. For example, the wind vectors in the Beaufort Sea in 1987 and 1988 have similar directions and were about as intense as those in 1998 but the open water areas during summer in the former were not as large as those in the latter. The direct effect of wind on the ice cover, however, is apparent in many cases. In 1995, for example, strong winds toward the Fram Strait probably caused the substantial reduction in the summer ice cover in the Kara and Barents Seas. Similar wind effects in 1981, 1991, and 1993 likely caused the large open water areas at the Siberian and Laptev Seas during the summer of these years. It is also apparent that the patterns for the wind vectors in 1999 is similar to those of 1998 and may explain similar summer ice covers during these 2 years. The summer ice covers are also similar in 1996 and 1984 when the average wind forcing at the periphery of the Arctic Basin is reduced to almost zero.

## 6. Changes in the Arctic Ocean Observed From Buoy Data

[31] Because of general inaccessibility, spatially and temporally detailed hydrographic measurements in the Arctic Ocean are rare if not unavailable. Significant changes in the ocean temperature structure over the past half-decade have been reported recently, using CTD data from ship and submarine cruises [e.g., Gunn and Muench, 2001]. In this study, we complement such previous observations with those observed continuously by the IOEB hydrographic (buoy) data at depths of 8, 45, and 75 m from April 1996 through December 1997 and at depths of 65 and 165 m from October 1997 to October 1998 (see Figure 1a). It is fortuitous that CTD measurements up to 500 m were also made on 27 April 1996 and 11 April 1997 at two adjacent locations. Although these measurements were originally meant to be used to check the calibration of the IOEB system, they actually provide useful information about the Arctic Ocean that is relevant to the anomalies observed. The measurements were not taken at exactly the same spot of the Arctic (see location in white dot adjacent to the label in Figure 1a), but they were made at generally the same bathymetry region and are close enough for a meaningful comparative analysis. The temperature and salinity profiles in Figure 13a show significant changes in the vertical structure of the ocean from 1 year to the other. The temperature profiles show a shallowing of the pycnocline with the temperature maximum of about  $-1.2^{\circ}\text{C}$  changing in depth from 76 to 45 m over the 2-year period (1996–1997). A slight warming in the upper ocean is also apparent. The salinity profiles (Figure 13a) show similar changes, with the average salinity near the surface changing from 30.3 to 29.3 psu and reflecting significant freshening in the water column close to the surface. Such a change suggests more ice melt in 1997 than in 1996, as indicated in Figure 3. However, the freshening can be caused in part by river runoff in the Mackenzie River, which was observed to be substantially larger in 1997 and 1998 than in 1996 or earlier years [Macdonald et al., 1999]. The circulation of such water in the Arctic Basin is affected by atmospheric circulation, thereby causing interannual variations of freshwater distribution in some regions [Ekwurzel et al., 2001]. It

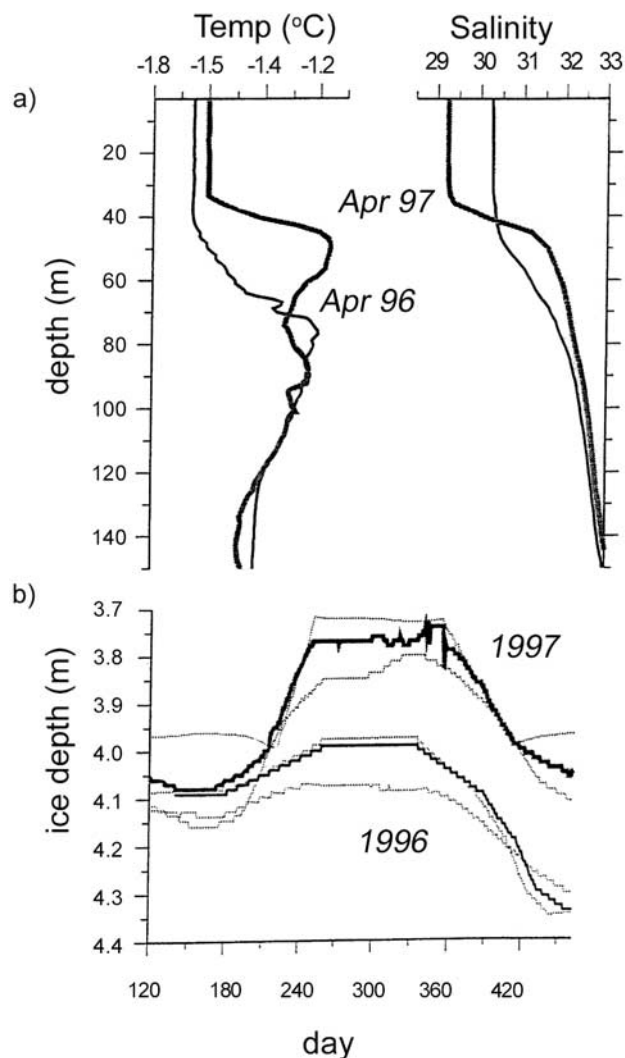


**Figure 13.** (a) Temperature and salinity profiles on 27 April 1996 at  $79^{\circ}\text{N}$  and  $139^{\circ}\text{W}$  (thin line) and on 11 April 1997 at  $77^{\circ}\text{N}$  and  $132^{\circ}\text{W}$  (bold line) and (b) ice thickness change from 1996 to 1997 (bold line for the best estimate and with the gray lines providing the possible range of values).

should be pointed out, however, that the river is more than 500 km away from the buoy location and the contribution might be minimal.

[32] The observed difference of temperature and salinity profiles in 1996 and 1997 (Figure 13a) is useful in the interpretation of the changing characteristics of the water mass as the IOEB drifted westward from 1996 to 1997. The feature of shallower halocline and thermocline in 1997, especially the structure of temperature maximum at the surface depth of 50 m, is commonly found in the western Beaufort Sea and in the Chukchi Sea, where the Bering Strait inflow modifies the water mass structure considerably. Changes of surface wind and oceanic current may have also played a role in the  $T$  and  $S$  changes. The cyclonic wind associated with the low msl pressure in 1996 may have intensified the transport of warmer water from the Bering Sea inflow to the Beaufort Sea and may have increased sea ice melting there. In fact, the sea ice thickness, inferred from

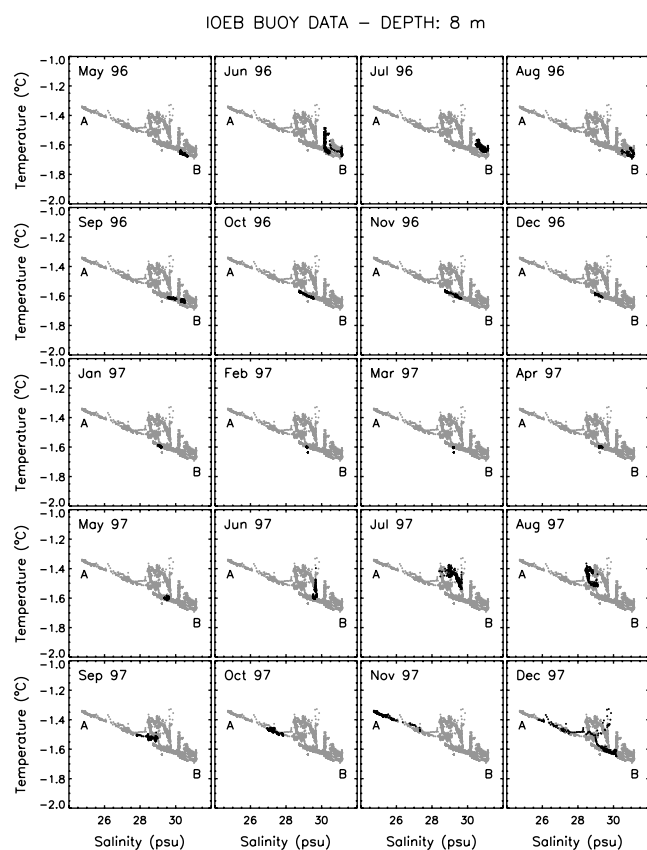


**Figure 14.**  $T$ - $S$  diagrams of daily temperature and salinity during each month (in black dots) at 8-m depth from May 1996 through December 1997 using IOEB data. The gray dots correspond to all the data available during the period.

IOEB observation of ice temperature, shows clearly a substantial thinning of the ice floe on which the IOEB platform was mounted (Figure 13b). This scenario of warm water advection and ice melting may have contributed to the change from a relatively cold and salty upper ocean in 1996 to a warmer and fresher one in 1997. This is consistent with more open water and ice melt in 1997 than in 1996, as illustrated in Figures 2 and 3. Alternatively, the difference between 1996 and 1997 may be primarily in the depth of penetrative convection. More effective convective entrainment prior to April 1996 could have caused the deeper mixed layer of higher salinity and deeper temperature maximum. The difference may thus reflect differences in storminess prior to freeze-up in the autumns of 1995 and 1996. The change may also reflect the difference in the strength of Ekman pumping between the 2 years, which influences isohaline depths.

[33]  $T$ - $S$  plots using the IOEB hydrographic data from 1996 through 1997 are shown on a month-to-month basis in Figures 14–16 for depths of 8, 45, and 75 m, respectively. In these plots, data points of temperature versus salinity from the entire data set are plotted as gray data points, with the observed values during each month represented by black dots. The month-by-month representation of the data provides the means to quantitatively assess seasonal and interannual changes in the ocean characteristics in  $T$ - $S$  space. It should be pointed out that the buoy is anchored

to an ice floe and it is the water column underneath this ice floe that is constantly being sampled by the string of sensors. Since the drift of the ice floe is not necessarily the same as that of the water mass underneath it, some of the changes in the measurements may be associated with the buoy going over different water mass regimes. The measurements can be viewed as divided into two parts. The first is the April 1996 to April 1997 period in which the buoy was almost stationary in the same general location (see Figure 1a). This provided the opportunity to investigate the seasonal characteristics of the ocean in a particular spot. The second part is after April 1997, in which both the IOEB and the SHEBA IOEB buoys were advected across the western region and provided a sampling of water mass over a large area. The shift in the drift velocity reflects the change in the atmospheric circulation from cyclonic to anticyclonic mode, as indicated earlier.

[34] The 8-m depth data set is presented in Figure 14, and as reference points in the discussion of the plots, the end points of the cluster of data have been labeled A and B. The line AB basically represents the relationship between the freezing temperature and the salinity value. A large part of the data set varies along this line, indicating that the water at this depth was near the freezing temperature in much of this period. There are some data points deviating from this line

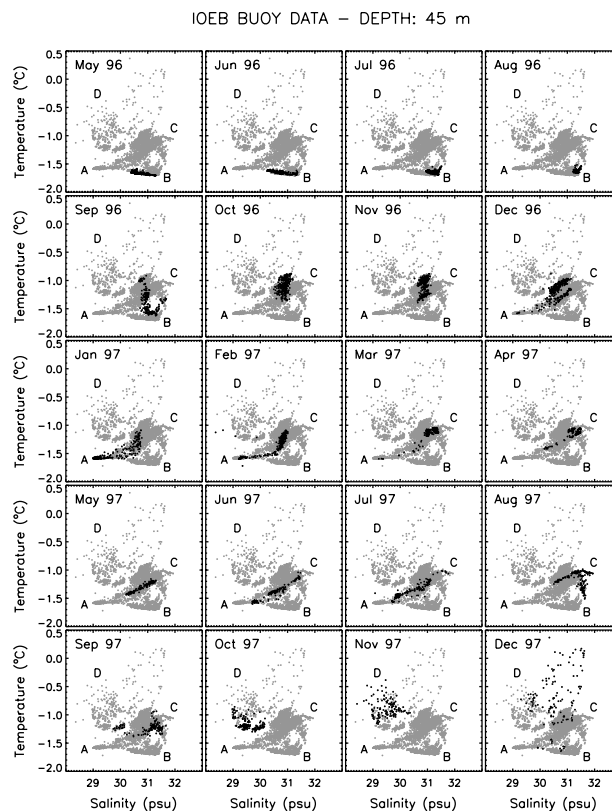


**Figure 15.**  $T$ - $S$  diagrams of daily temperature and salinity during each month (in black dots) at 45-m depth from May 1996 through December 1997 using IOEB data. The gray dots correspond to all the data available during the period.

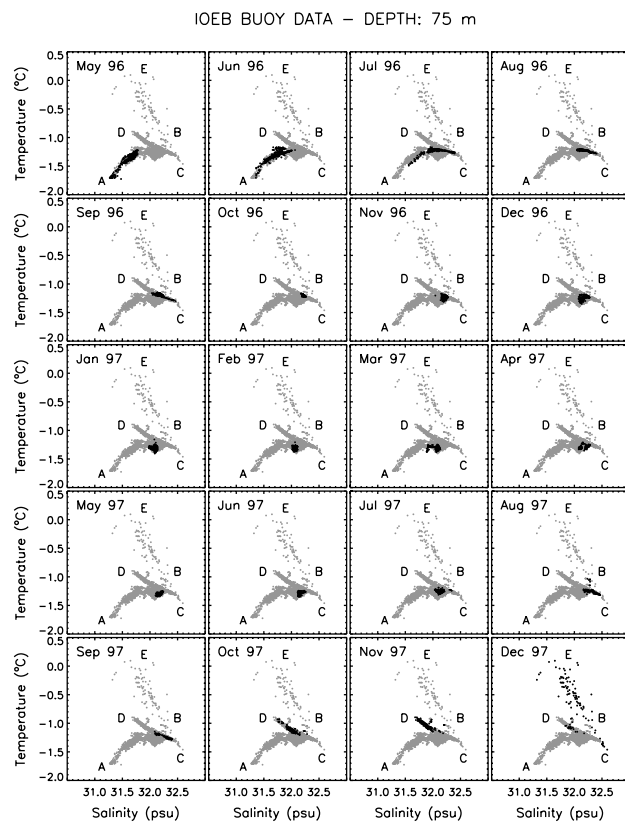


**Figure 16.**  $T$ - $S$  diagram of daily temperature and salinity during each month (in black dots) at 75-m depth from May 1996 through December 1997 using IOEB data. The gray dots correspond to all the data available during the period.

and they occurred mostly in the summer season (June–August in 1996 and June–September in 1997). This simply indicates that the oceanic mixed layer in the summer season was warmed to above the freezing point due to enhanced solar radiation. The only deviation that occurred in a non-summer month was December 1997. The warming was due to a strong and deep mixing, with the thermocline water driven by a powerful storm [Yang *et al.*, 2001].

[35] It is apparent that in May 1996, the data during the month are very well defined and close to the highest salinity value. In June 1996, the values were much more variable, becoming less saline and warmer at first and then getting colder and more saline after that. The higher temperature values may have been caused by the presence of warm core eddies in the vicinity, as has been observed by Gunn and Muench [2001], but since similar effects are not observed at other depths, this may be unlikely. In July, the values were basically the same as the previous month but a slight warming is apparent that may reflect the seasonal warming. In August 1996, a slight cooling is observed and the salinity is at its highest value during the entire measurement period. In September–December, the data points are very confined within the AB line, indicating a gradual freshening and a slight increase in temperature. The values are almost constant thereafter from January through April 1997. In May, there is a slight increase in salinity, while in June there is a

substantial increase in temperature that again reflects seasonal warming. In the summer (June, July, and August), the water mass was again in its most saline state during the year (except in December, which is a special case, as mentioned earlier). It is also apparent that the salinity is significantly less than in August 1996. However, most of the data points are above the AB line, indicating significant warming of the water mass. This occurred despite calmer winds in the region than what occurred in previous months, as indicated in Figure 11. In September, the data points are again mainly along AB and went through considerable freshening and warming in the October and November period. In December 1997, the data points slide toward higher salinity along the line AB, but at some time period, the values are significantly above the line. It is apparent that the data points are more confined to a certain location in 1996 than in 1997. This may be partly caused by different wind directions in 1996, as indicated in the previous section, compared to 1997. In December 1997, the storm event reported by Yang *et al.* [2001] is the primary reason for some of the abnormal redistribution of the data points. Comparing data for the same months, the water mass observed in 1996 is shown to be always colder and more saline than that of 1997. The buoy was in the same general area until at least August 1997.

[36] The 45-m data in Figure 15 show that there is a lot more variability in the physical properties of the ocean at this depth than at 8 m. The greater variability at this location is expected because it is the approximate depth of the halocline and thermocline, as indicated in Figure 13a. The large vertical gradients of temperature and salinity associated with the halocline and thermocline make  $T$  and  $S$  more sensitive to external forcing such as vertical mixing. The  $T$ - $S$  diagrams are shown with labels of A, B, C, and D, which are again used to describe redistribution of data points with time. In general, the data points appear to move linearly with time and along AB or along AC, but during other times, the data points deviate substantially from these lines, especially toward the end of 1997. The salinity and temperature values were well defined in April 1996 (not shown but see Figure 13a). The salinity tends to increase from May to August 1996 as the values move along the line AB. As in the 8-m data, the water mass gets its coldest and most saline values during the year in July and August 1996. Then in September–November, the temperatures became significantly warmer, while salinities were generally less than 31 psu. This may in part be due to atmospheric forcing since at about the same time period, the wind vectors change direction, as indicated in Figure 11. In December, a general cooling and freshening ensued, and this event continued through February 1997. In March–July 1997, the data points are confined along AC, showing basically slight increases in salinity and temperature. The water mass reaches its most saline value during the year again in August 1997, but the average salinity is lower than in August 1996 only because the values during the month are more spread out. In August and early September 1997, some of the data points follow a totally different pattern and are confined between C and B, but from September through December, the data points each day varied by quite a lot and show a drastic decrease in salinity. The wind vectors in Figure 11 show cyclonic circulation during this time. Again, this later period is associated with a storm in the region, as detected

by the buoy wind data and reported by *Yang et al.* [2001]. As in the 8-m data, the water mass observed for the same months was again colder and more saline in 1996 than in 1997.

[37] At 75-m depth, the IOEB *T-S* data, as depicted in Figure 16, show more defined characteristics of the water mass than at 45 m. In April 1996, the data points during the month are confined to a small cluster (not shown but see Figure 13a as reference). Then from May to June 1996, there was significant warming accompanied by increases in salinity that went on up through September. The values for temperature and salinity then became very well defined in October 1996 through July 1997. After that, the data indicate increasing temperatures and slight freshening up to November 1997, but in December 1997, the data show high salinity but very variable temperature. The latter indicates that the effect of the reported storm [*Yang, 2001*] was at least as deep as 75 m. Comparing the measurements for the same months of 1996 and 1997, the reverse to what was observed at depths of 8 and 45 m is apparent. This is because of the crossing of the salinity and temperature profiles before this depth, as shown in Figure 13a. Month-to-month changes are, however, apparent, suggesting changes in the structure and location of the pycnocline.

[38] The IOEB data show generally warmer and fresher water in 1997 than in 1996 near the surface at 8 m, while at 45 and 75 m, the water was warmer and more saline. These results are consistent with the results from the more detailed CTDs in April 1996 and April 1997. The fresher water near the surface is suggestive of more ice melting in 1997 compared to that in 1996. IOEB ice depth data are compared in Figure 13b for 1996 and 1997, and it is apparent that the ice thickness decreased substantially from one year to the other. The warmer water may be related to the larger open water area in 1997 that likely caused an increase in the solar heating of the mixed layer.

[39] Since the IOEB went to shallow waters in 1998, the ocean measurements from this sensor are more difficult to interpret as a continuation of the time series. For completeness, the results from the SHEBA IOEB from October 1997 through October 1998 which were taken at 65-m depth are shown in Figure 17. The only IOEB data that can be compared directly with these data are those of Figures 15 and 16. This buoy was deployed at generally the same water mass region as that of IOEB, but the characteristics of the water may not be exactly the same and the measurements at 65-m depth may not match those at 75 m for the other buoy, especially near the pycnocline. The *T-S* data at 65-m depth are shown in Figure 17a. Significant activity occurred in January–March 1998, but overall, the change was toward more saline and colder water. Comparing these plots with those of Figure 16 (for 75-m measurements), it is apparent that the data points along AB in Figure 17a correspond to data points along CD in Figure 16 during the overlap period in October and November 1997. A warming episode occurred at 75 m (Figure 16) in December 1997, but this event was not observed in the 65-m data (Figure 17a) until January–March 1998. It should be pointed out that the buoy went through significant change in bathymetry during these periods (see Figure 1a). Generally, the water was cooler and slightly more saline in 1998 than in 1997 (and 1996) at this depth.

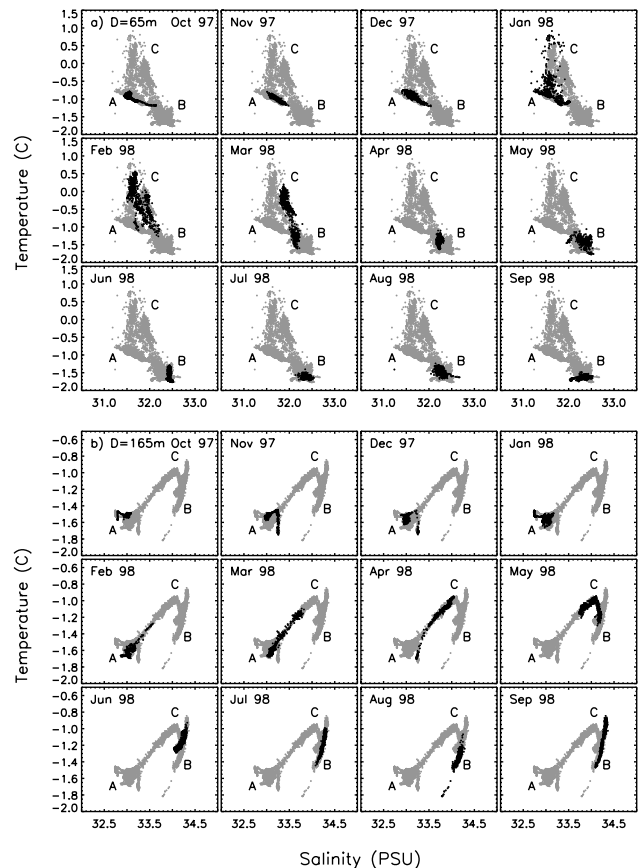


**Figure 17.** (a) *T-S* diagrams of daily temperature and salinity during each month (in black dots) at 65-m depth from October 1997 through September 1998 using SHEBA IOEB data and (b) *T-S* diagram of daily temperature and salinity during each month (in black dots) at 165-m depth from October 1997 through September 1998 using SHEBA IOEB data. The gray dots correspond to all the data available during the period.

[40] *T-S* plots at a depth of 165 m are generated from SHEBA IOEB data and presented in Figure 17b to evaluate temporal changes deeper in the ocean. From October 1997 to January 1998, the data points are basically confined in the same cluster. From February through May 1998, the water mass apparently became warmer and more saline, with the data points migrating from location A to location C along almost a straight line. Again, part of the changes may be associated with changes in the bathymetry (Figure 1a). From June through September 1998, the data points are confined along a different cluster CB that might represent a different water mass regime. During this period, the water mass was warmer and more saline than the October 1997 data. The warmer upper layer is consistent with more solar heating due to more open water in 1998 than in 1997.

[41] The *T-S* data set from the buoys provides new insights into the seasonal and interannual variability of the ocean that may be associated with the observed variability in the ice cover. A seasonal cycle in both salinity and temperature is apparent, especially from the 1996 data. This means that water sampling should take this seasonality into

consideration when interannual changes in water mass properties are being studied. It is intriguing to observe that at the depths sampled, the coldest and most saline water generally occur during the summer. This phenomenon is counterintuitive to what is expected during the melt season and is an indication that there is much more to learn about Arctic processes. The cause is likely not due to the drifting of the buoy into a high-salinity area since it happened every year during the study period. A possible explanation is upwelling from deeper ocean layers due to less wind convergence, which is typical for the summer (A. Proshutinsky, personal communication, 2002).

[42] The buoy drift, as shown in Figure 1a, indicates that there was a substantial change in ice dynamics from 1996 to 1997 associated with the change in atmospheric circulation, as indicated earlier. Changes in oceanic dynamics could lead to the advection of warm water and vertical mixing and thus changes in heat and salinity fluxes. The Beaufort and Chukchi Seas are known to be strongly influenced by the inflow of Bering seawater which is considerably warmer than the surface water in the Arctic. This warmer water was evident in the temperature profile shown in Figure 13a at the depth of 40 m. This warmer water, sitting just 30–40 m below the surface, is a large reservoir of heat that can have a profound impact on the heat content in the mixed layer. An example for this occurred in December 1997 when a strong storm forced a deep mixing that brought up this warm water to the surface and melted sea ice considerably in the vicinity of IOEB [Yang *et al.*, 2001]. It is also interesting to note that the strong alongshore wind in the Beaufort Sea in 1997 and 1998 may have also forced upwelling along the coast, which could be an effective way of bringing warm water to the surface. The wind condition in 1996 was not favorable for upwelling in the same region.

[43] Solar radiation through open water areas in the summer is a major source of heat for the Arctic Ocean mixed layer [Maykut and McPhee, 1995] since the albedo of water is much lower than that of ice. The presence of a large open water area within the pack significantly alters the characteristics of the mixed layer in the Arctic. A warming in the latter would in turn cause further increase in open water area, as in 1998. McPhee *et al.* [1998] suggested a different scenario in that a generally more cyclonic circulation would dynamically reduce ice concentration, allowing more solar radiation to enter the upper ocean through increased open water area. This apparently did not happen in 1996 when the atmospheric circulation was cyclonic.

## 7. Long-Term Trends in Surface Air Temperatures and Ocean Hydrography

[44] Since the observed variability and trends in the ice cover, surface temperature, and ocean hydrography are based on relatively short record lengths, it would be of interest to find out how these results compare with those from much longer time series data. Monthly anomalies derived from surface air temperature data from the few stations with record lengths of 100 years (or more as compiled by Jones *et al.* [1999]) in the Arctic and located  $>50^{\circ}\text{N}$  are shown in Figure 18a. Linear regression of the data points indicates that surface air temperature in the region has been going up at about  $0.07^{\circ}\text{C}$  per decade. This

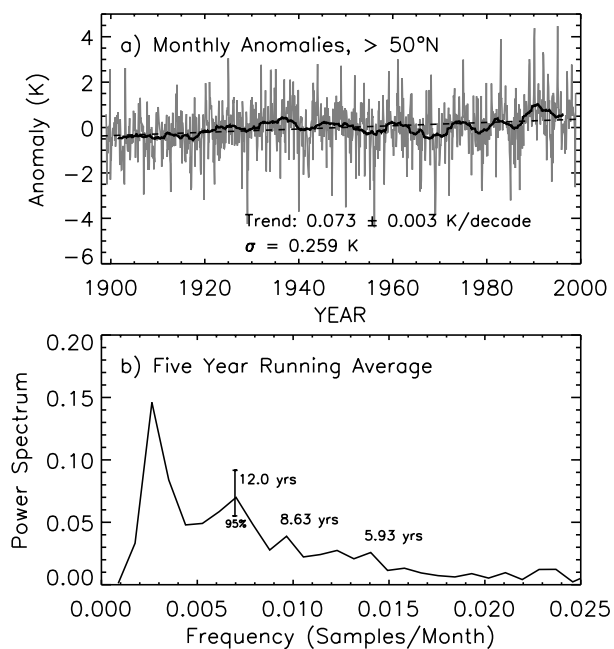


**Figure 18.** (a) Observed long-term changes in monthly surface air temperature and 5-year running average (in bold black) and (b) the results of spectral analysis of a 5-year running mean of the data in Figure 18a.

is significantly higher than that of global averages, but the trend from a 19-year subset of data from the same stations shows a much larger trend of  $0.38^{\circ}\text{C}$  per decade. The corresponding trend from the 19-year satellite data over the entire sea ice-covered area was slightly higher at  $0.44^{\circ}\text{C}$  per decade. The satellite data do not have the same measurement accuracy as the station data but long-term temperature data in the central Arctic are basically nonexistent, and most of the stations with temperature records of 100 years or more are but a few, located mainly in Europe and northern Russia. Where there are station data, the satellite data compare very well with station data. Figure 18a also shows the 5-year running mean of the 100-year temperature record showing a fluctuation with some periodic cycle, especially in the 1970s through 1990s. During the latter period, peak values occurred in 1982 and 1990, which are years when the ice area for the entire Arctic had anomalously low values. A warming is also apparent from the trend line, the rate being  $0.074 \pm 0.003$  K per decade. A power spectrum plot from a Fourier analysis of the 5-year running mean is shown in Figure 18b and indicates a peak at about 12 years. The vertical line adjacent to the 12-year peak is the 95% confidence level for the 12-year cycle. This peak is close to the 10-year periodicity observed from the open water distribution, as discussed earlier.

[45] To gain additional insight into the long-term changes in the characteristics of the ocean in the region, available hydrographic data in the Beaufort Sea have been assembled and are used to depict historical water mass properties at five depths (10, 40, 70, 110, and 160 m) and to assess interannual changes. This was done through comparison with data from the Environmental Working Group's (EWG) optimally

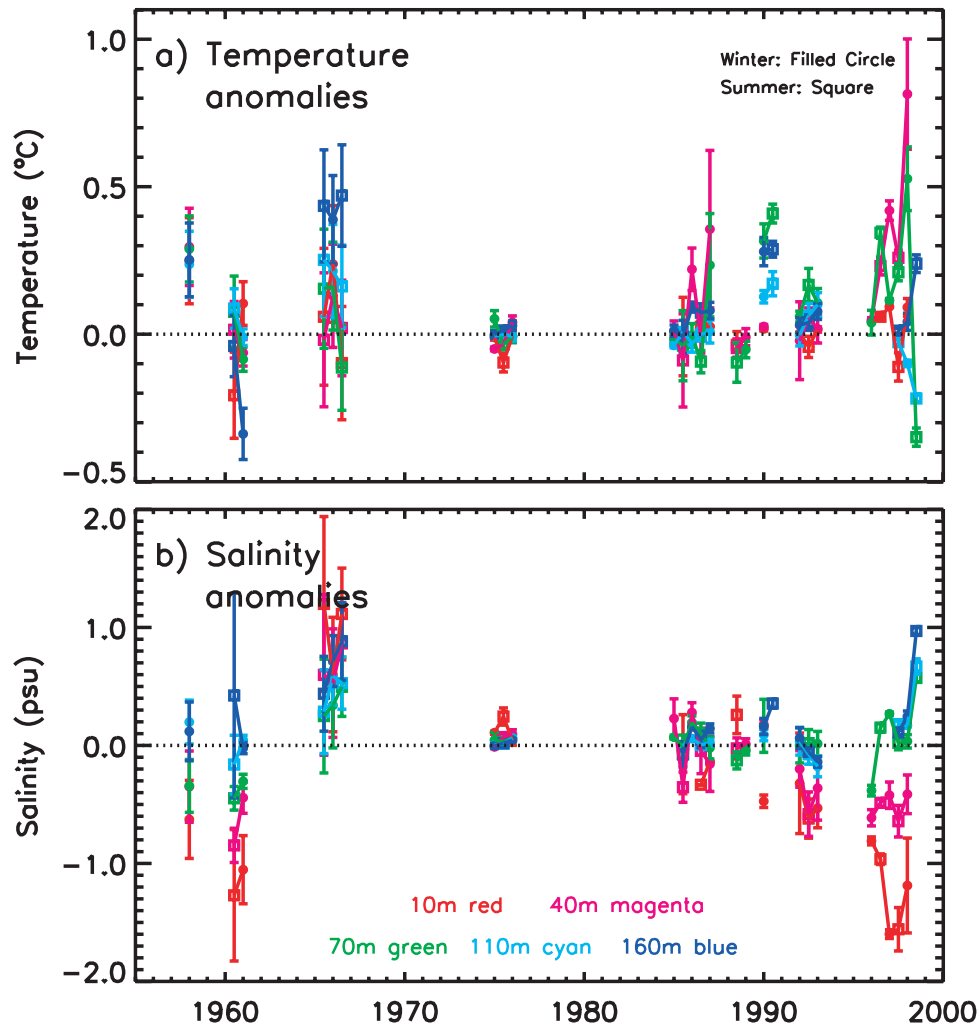


**Figure 19.** Observed anomalies at five depths (10, 40, 70, 110, and 160 m) in the Beaufort Sea from 1955 to 1998. EWG data were subtracted from data from T3/Arlis, SALARGOS, and IOEB.

interpolated hydrographic atlas of the Arctic Ocean. Synoptic air, ice, and ocean interactions may cause significant variations in hydrographic properties in the surface layer of the ocean, causing short-term bias in individual hydrographic measurements at any discrete time. Consequently, only data sets in which the time series of profiles had frequent measurements made for several months were analyzed. In the Beaufort Sea, these consist of ice camp data from ice island T3 (1958 and 1965–1966), Arlis (1960–1961), and Arctic Ice Dynamics Joint Experiment (AIDJEX) (1975–1976), and data from six SALARGOS buoys (between 1985 and 1993) and two IOEBs (1996–1998). Figure 1a shows the locations of the last three. The frequency of the ice camp measurements is generally two per day or less, while the buoys obtain data 10 times more frequently, which makes the later data sets more statistically robust. In addition, errors associated with the raw measurements improved from about  $\pm 0.1^\circ\text{C}$  and  $\pm 0.03$  psu before AIDJEX to about  $\pm 0.03^\circ\text{C}$  and  $\pm 0.03$  psu during AIDJEX. The accuracies of the instrumentation of current buoys are as good as  $\pm 0.02^\circ\text{C}/\text{yr}$  and  $\pm 0.001$  psu (S/m/month).

[46] The ice camp and buoy observations are roughly bounded by latitude from  $72^\circ\text{N}$  to  $80^\circ\text{N}$  and  $30^\circ\text{W}$  to

$170^\circ\text{W}$  (see Figure 1a) but occupy different periods in time and space between 1958 and 1998. To study trends in the ocean variables, anomaly time series were created by removing seasonal variations on a station-by-station basis using the spatially interpolated EWG data, as mentioned above (which we now refer to as EWG climatologies), at the corresponding grid point for either summer (June–November) or winter (December–May) seasons. The EWG climatology is constructed from U.S. and Russian data obtained between 1948 and 1993 from drifting stations, icebreakers, and drifting buoys, and contains average temperature and salinities for winter and summer seasons, with a horizontal resolution of 50 km and vertical spacing of 10 m. While the atlas provides a long-term three-dimensional (3-D) estimate of hydrographic properties, plots of the station distribution by decades clearly show that the greatest spatial coverage in the Canada Basin was primarily from Russian data in the 1970s. The time series of anomalies are then averaged by summer or winter, producing 40 seasons of upper ocean hydrographic anomaly determinations, as shown in Figure 19. The statistical errors in the seasonal means are generally less than  $0.1^\circ\text{C}$  and 0.25 psu for temperature and salinity, respectively.

[47] The hydrographic data from five AIDJEX ice camps (see small black circles, Figure 1a) show good consistency with the EWG climatology in 1975–1976, displaying only a few temperature anomalies greater than  $0.1^{\circ}$  and a single salinity anomaly greater than 0.5 psu (all in the summer mixed layer). SALARGOS buoy data (see white line, Figure 1a) between 1985 and 1989 also agree with the EWG climatology, except for elevated temperatures in one, which are associated with high statistical error. After 1989, however, significant freshening in the mixed layer and warming in the upper halocline are observed. SALARGOS buoy data indicate that the season-average salinity at 10 m is 0.5–0.6 psu less than the EWG between 1990 and 1993. IOEB buoy data follow the trend in 1996 and 1997 and with the detected anomalies increasing from 1.0 to 1.5 psu. Concurrently, temperature differences at depths of 70, 110, and 160 m increased by  $0.2^{\circ}$ – $0.4^{\circ}\text{C}$  in 1990 but receded in 1992 and 1993. From summer 1996 through winter 1998, the temperature anomalies at 70 m again increased by  $0.2^{\circ}$ – $0.4^{\circ}\text{C}$ , but at 110 m, the temperature anomaly receded in the winter of 1997 to  $0.1^{\circ}\text{C}$  between high values of  $0.3^{\circ}\text{C}$  in 1996 and  $0.6^{\circ}$ – $0.7^{\circ}\text{C}$  from 1997 to 1998. This indicates a significant decrease in mixed-layer density and an increase in stratification after 1989. While the upper halocline warms, the near-surface temperature elevation above freezing remains nearly constant, presumably due to surface processes.

[48] These computations indicate that the AIDJEX stations in 1975–1976 and SALARGOS buoys in 1985–1989 show the least variation from the EWG climatology at all depths, which is consistent with the EWG sampling bias in the 1970s. On the other hand, a statistically significant freshening of the near-surface water and the elevation of the upper halocline temperature in the central Beaufort Sea is apparent after 1989, confirming previous results of *Melling* [1998], *Newton and Sotirin* [1997], and *McPhee et al.* [1998]. Temperatures at 70 and 110 m show a significant increase of  $0.7^{\circ}\text{C}$  over the climatology, while mixed layer remains near freezing. The timing is consistent with the large increase in sea ice melt reported by *MacDonald et al.* [1999] and could be related to the cyclonic sea level pressure pattern and the Arctic Oscillation [*Thompson and Wallace*, 1998]. Significant negative anomalies at 10 m are observed in the summer of 1992 and in winter of 1997, with the anomaly value exceeding 1.5 psu in 1997. These peaks appear to precede peaks of anomalously low ice concentration by about 1 year and also lag changes in transport through the Bering Strait [*Roach et al.*, 1995] by about 3 years.

## 8. Discussion and Conclusions

[49] Available sea ice, ocean, and atmospheric surface data have been used in this study to gain insights into the observed changes in the Arctic in the 1990s. The synergy of different geophysical observable in the Arctic region is apparently very strong. The retreat of sea ice during the 1996–1998 period in the Beaufort Sea is studied and shown to be coherent with warming episodes in both the atmosphere and the ocean in the region and with changing wind and pressure patterns. Detailed CTD measurements 1 year apart in approximately the same water mass region also show a freshening and a warming in the upper ocean layer

from 1996 to 1997. This is compatible with more melted ice (or more river runoff) and warmer temperatures in 1997 than in 1996, as suggested by other data sets.

[50] The distributions of open water area in the western and eastern sectors of the Arctic have been quantified separately to better understand the ice retreat in relation to ice dynamics and its circulation patterns. The open water distributions exhibit an approximately decadal variability but with one sector lagging the other by about 3 years. This suggests that the variability is driven at least in part by an atmospheric forcing likely associated with the Arctic Oscillation and the North Atlantic Oscillation [*Thompson and Wallace*, 1998; *Mysak*, 1999]. Such periodic variability is interrupted only by the big anomalies like those in 1993 and 1998 in the western sector and in 1995 in the eastern sector. It is these big anomalies that were mainly responsible for the negative trends in ice cover and positive trends in surface temperatures in the last two decades, especially because the anomalies tended to be larger and more prevalent in the 1990s than in the 1980s.

[51] Spatially detailed surface temperatures from satellite infrared data enabled the assessment of regional effects of warming and the spatial scope of the anomalies that usually extend beyond the sea ice cover boundaries. The occurrence in 1998 of the largest area of exposed water ever observed in the Beaufort Sea region by satellite data was concurrent with large temperature anomalies in the western sector and in North America. It is interesting that in some other areas, like Russia and the Laptev Sea, there was actually a slight cooling going on. This is indicative of the complexity of the Arctic climate system and the difficulty of making accurate interpretations of available station data, which are so sparsely distributed.

[52] The changing wind patterns have also been shown to be a significant factor affecting the ice variability. The period from 1996 to 1997 corresponded to a change from cyclonic to anticyclonic wind circulation. Such circulation may have caused a mass transport of multiyear ice from the western sector to the eastern sector that may have facilitated the formation of large areas of open water in the Beaufort Sea in 1997 and 1998. The anticyclonic wind is the favorable direction for transporting some of the ice floes to the warmer part of the Arctic Ocean, like the Chukchi Sea, where they melt. The anticyclonic wind also forces divergence of sea ice from the land-sea boundary toward the central Arctic Basin. Furthermore, the prevailing anticyclonic wind forces upwelling along the boundary. Because the thermocline in the Arctic Ocean is very shallow, the wind-driven upwelling can be effective for upward heat flux to the mixed layer. When the ice cover is opened by wind and oceanic current, solar radiation increases and provides a positive feedback to further reduce the extent of the ice cover.

[53] However, the result of analysis of 7-month average wind data from 1979 to 1999 indicates that changes in wind circulation had occurred several times in the past (e.g., 1987 and 1988) but were not always accompanied by abnormally large open water areas such as those in 1997 and 1998. The anticyclonic circulation appears to be the pattern that is more conducive to the occurrences of large open areas in the western region but it is also the more prevalent.

[54] The role of the Arctic Ocean in the changing Arctic climate system is also studied using available oceanographic

data. Detailed CTD hydrographic measurements in April 1996 and April 1997 in approximately the same area in the central Beaufort Sea also show a shallowing of the pycnocline from about 80 to 45 m, a change in salinity of the upper 30-m layer from 30.2 to 29.2 psu, while the upper layer temperature increased from  $-1.61^{\circ}$  to  $-1.55^{\circ}\text{C}$ . Continuous IOEB data at 8, 45, and 75 m show similar changes for the 1996–1997 period, while the SHEBA IOEB data show similar effects at slightly different depths from 1997 to 1998. These results are consistent with more ice melt at the latter years that may be associated with a thinning and retreating ice cover. Available historical data from 1957 to the present also indicate that the anomalies in ocean temperature and salinity in the Beaufort Sea in 1997 and 1998 were unusually large compared to previous years. This study shows that much of the observed trends in the ice cover and temperature are associated with big anomalies in these variables in the 1990s. The biggest anomaly in open water area in the Beaufort Sea observed by satellites occurred in 1998. This occurred concurrently with a big positive anomaly in surface temperature and a strong anticyclonic wind circulation in the same general region. It also occurred concurrently with a freshening and warming of the upper layer of the ocean and the occurrence of an extra polar ENSO event. The direct relationships between some of these variables have been quantified but longer data records coupled with in-depth modeling studies are needed to establish the real cause of the observed anomalies.

[55] **Acknowledgments.** We would like to acknowledge with gratitude the excellent programming and analysis support provided by Robert Gerstein of SSAI and Larry Stock of Caelum Research Inc. EWG Atlas (including SALARGOS buoy data) and ADJEX ice camp data were provided by the National Snow and Ice Data Center of the University of Colorado. Deployments of the IOEB were supported by the Japanese Marine Science and Technology Center (JAMSTEC). In particular, we thank T. Takizawa and K. Hatakeyama for their long-term collaboration in the IOEB project. This project was supported by the NASA Cryosphere Program and the NASA Earth Science Enterprise Project.

## References

- Aagaard, K., and E. Carmack, The Arctic Ocean and climate: A perspective, in *The Polar Oceans and Their Role in Shaping the Global Environment*, *Geophys. Monogr. Ser.*, vol. 85, edited by O. M. Johannessen, R. D. Muench, and J. E. Overland, pp. 5–20, AGU, Washington, D. C., 1994.
- Aagaard, K., et al., U.S. Canadian researchers explore Arctic Ocean, *Eos Trans. AGU*, 77, 209–213, 1996.
- Bjorgo, E., O. M. Johannessen, and M. W. Miles, Analysis of merged SSMR-SSM/I time series of Arctic and Antarctic Sea ice parameters 1978–1995, *Geophys. Res. Lett.*, 24, 413–416, 1997.
- Budyko, M. I., Polar ice and climate, in *Proceedings of the Symposium on the Arctic Heat Budget and Atmospheric Circulation*, RM 5233-NSF, edited by J. O. Fletcher, pp. 3–21, Rand Corp., Santa Monica, Calif., 1966.
- Burroughs, W. J., *The Climate Revealed*, 192 pp., Cambridge Univ. Press, New York, 1999.
- Carmack, E. C., R. W. Macdonald, R. G. Perkin, F. A. McLaughlin, and R. J. Pearson, Evidence of warming of Atlantic water in the southern Canadian Basin of the Arctic Ocean: Results from the Larson-93 expedition, *Geophys. Res. Lett.*, 22, 1061–1064, 1995.
- Comiso, J. C., Variability and trends in Antarctic surface temperatures from in situ and satellite infrared measurements, *J. Clim.*, 13, 1674–1696, 2000.
- Comiso, J. C., Satellite observed variability and trend in sea ice extent, surface temperature, albedo, and clouds in the Arctic, *Ann. Glaciol.*, 33, 457–473, 2001.
- Comiso, J. C., A rapidly declining perennial sea ice cover in the Arctic, *Geophys. Res. Lett.*, 29(20), 1956, doi:10.1029/2002GL015650, 2002.
- Comiso, J. C., and R. Kwok, The summer Arctic Sea ice cover from satellite observations, *J. Geophys. Res.*, 101, 28,397–28,416, 1996.
- Comiso, J. C., D. Cavalieri, C. Parkinson, and P. Gloersen, Passive microwave algorithms for sea ice concentrations, *Remote Sens. Environ.*, 60, 357–384, 1997.
- Ekwurzel, B., P. Schlosser, R. A. Mortlock, R. G. Fairbanks, and J. H. Swift, River runoff, sea ice meltwater, and Pacific water distribution and mean residence times in the Arctic Ocean, *J. Geophys. Res.*, 106, 9075–9092, 2001.
- Gloersen, P., W. Campbell, D. Cavalieri, J. Comiso, C. Parkinson, and H. J. Zwally, Arctic and Antarctic Sea ice, 1978–1987: Satellite passive microwave observations and analysis, *NASA Spec. Publ.*, 511, 290 pp., 1992.
- Gunn, J. T., and R. D. Muench, Observed changes in Arctic Ocean temperature structure over the past half decade, *Geophys. Res. Lett.*, 28, 1035–1038, 2001.
- Honjo, S., T. Takizawa, R. Krishfield, J. Kemp, and K. Hatakeyama, Drifting buoys make discoveries about interactive processes in the Arctic Ocean, *Eos Trans. AGU*, 76, 209–215, 1995.
- Jones, P. D., M. New, D. E. Parker, S. Martin, and I. G. Rigor, Surface air temperature and its changes over the past 150 years, *Rev. Geophys.*, 37, 173–199, 1999.
- Krabill, W. C., E. Frederick, E. S. Manizade, C. Martin, J. Sonntag, R. Swift, R. Thomas, W. Writhe, and J. Yungel, Rapid thinning of parts of the southern Greenland ice sheet, *Science*, 283, 1522–1524, 1999.
- Krishfield, R., S. Honjo, T. Takizawa, and K. Hatakeyama, Ice-Ocean Environmental Buoy Program: Archived data processing and graphical results from April 1992 through November 1998, *Tech. Rep. WHOI-99-12*, 83 pp., Woods Hole Oceanogr. Inst., Woods Hole, Mass., 1999.
- Kwok, R., J. C. Comiso, and G. Cunningham, Seasonal characteristics of the perennial ice cover of the Beaufort Sea, *J. Geophys. Res.*, 101, 28,417–28,439, 1996.
- Kwok, R., A. Schweiger, D. A. Rothrock, S. Pang, and C. Kottmeier, Sea ice motion from satellite passive microwave data assessed with ERS and buoy motions, *J. Geophys. Res.*, 103, 8191–8214, 1998.
- Lindsay, R. W., Temporal variability of the energy balance of thick Arctic pack ice, *J. Clim.*, 11, 313–333, 1998.
- Macdonald, R. W., E. C. Carmack, F. A. McLaughlin, K. K. Falkner, and J. H. Swift, Connections among ice, runoff, and atmospheric forcing in the Beaufort gyre, *Geophys. Res. Lett.*, 26, 2223–2226, 1999.
- Manabe, S., M. J. Spelman, and R. J. Stoufer, Transient responses of a coupled ocean-atmosphere model to gradual changes of atmospheric CO<sub>2</sub>, part II, Seasonal response, *J. Clim.*, 5, 105–126, 1992.
- Maykut, G. A., and M. G. McPhee, Solar heating of the Arctic mixed layer, *J. Geophys. Res.*, 100, 24,691–24,703, 1995.
- McPhee, M. G., T. P. Stanton, J. H. Morison, and D. G. Martinson, Freshening of the upper ocean in the Arctic: Is perennial sea ice disappearing?, *Geophys. Res. Lett.*, 25, 1729–1732, 1998.
- Melling, H., Hydrographic changes in the Canada Basin of the Arctic Ocean, 1979–1996, *J. Geophys. Res.*, 103, 7637–7645, 1998.
- Morison, J., M. Steele, and R. Anderson, Hydrography of the upper Arctic Ocean measured from the nuclear submarine USS Pargo, *Deep Sea Res., Part 1*, 45, 15–38, 1998.
- Mysak, L. A., Interannual variability at northern high latitudes, in *Beyond El Niño: Decadal and Interdecadal Climate Variability*, edited by A. Navarra, pp. 1–24, Springer-Verlag, New York, 1999.
- Mysak, L. A., and S. A. Venegas, Decadal climate oscillations in the Arctic: A new feedback loop for atmosphere-ice-ocean interactions, *Geophys. Res. Lett.*, 25, 3607–3610, 1998.
- Newton, J. L., and B. J. Sotirin, Boundary undercurrent and water mass changes in the Lincoln Sea, *J. Geophys. Res.*, 102(C2), 3393–3403, 1997.
- Parkinson, C. L., D. J. Cavalieri, P. Gloersen, H. J. Zwally, and J. C. Comiso, Arctic Sea ice extents, areas, and trends, 1978–1996, *J. Geophys. Res.*, 104, 20,837–20,856, 1999.
- Perovich, D. K., B. C. Elder, and J. A. Richter-Menge, Observations of the annual cycle of sea ice temperature and mass balance, *Geophys. Res. Lett.*, 24, 555–558, 1997.
- Proshutinsky, A., and M. Johnson, Two circulation regimes of the wind-driven Arctic Ocean, *J. Geophys. Res.*, 102, 12,493–12,514, 1997.
- Rigor, I. G., J. M. Wallace, and R. I. Colony, Response of sea ice to the Arctic Oscillation, *J. Clim.*, 15, 2648–2663, 2002.
- Roach, A. T., K. Aagaard, C. H. Pease, S. A. Salo, T. Weingartner, V. Pavlov, and M. Kulakov, Direct measurements of transport and water properties through the Bering Sea, *J. Geophys. Res.*, 100, 18,443–18,457, 1995.
- Rothrock, D. A., Y. Yu, and G. A. Maykut, Thinning of the Arctic Sea-ice cover, *Geophys. Res. Lett.*, 26, 3469–3472, 1999.
- Steele, M., and J. H. Morison, Hydrography and vertical fluxes of heat and salt northeast of Svalbard in autumn, *J. Geophys. Res.*, 98, 10,013–10,024, 1993.

- Steffen, K., and J. E. Box, Surface climatology of the Greenland ice sheet: Greenland climate network, 1995–1999, *J. Geophys. Res.*, *106*, 33,951–33,964, 2001.
- Steffen, K., et al., Snow and ice applications of AVHRR in polar regions, *Ann. Glaciol.*, *17*, 1–16, 1993.
- Thompson, D. W. J., and J. M. Wallace, The Arctic Oscillation signature in the wintertime geopotential height and temperature fields, *Geophys. Res. Lett.*, *25*, 1297–1300, 1998.
- Thorndike, A. S., and R. Colony, Sea ice motion in response to geostrophic winds, *J. Geophys. Res.*, *87*, 5845–5852, 1982.
- Wadhams, P., Evidence of thinning of the Arctic ice cover north of Greenland, *Nature*, *345*, 795–797, 1988.
- Wadhams, P., and N. R. Davis, Further evidence of ice thinning in the Arctic Ocean, *Geophys. Res. Lett.*, *27*, 3973–3976, 2000.
- Walsh, J. E., W. L. Chapman, and T. L. Shy, Recent decrease of sea level pressure in the central Arctic, *J. Clim.*, *9*, 480–486, 1996.
- Yang, J., J. C. Comiso, R. Krishfield, and S. Honjo, Role of synoptic storms in the development of the 1997 warming and freshening event in the Beaufort Sea, *Geophys. Res. Lett.*, *28*, 799–802, 2001.
- Zhang, J., D. Rothrock, and M. Steele, Recent changes in Arctic Sea ice: The interplay between ice dynamics and thermodynamics, *J. Clim.*, *13*, 3099–3114, 2000.

---

J. C. Comiso, Laboratory for Hydrospheric Processes, NASA Goddard Space Flight Center, Greenbelt, MD 20771, USA. (comiso@joey.gsfc.nasa.gov)

S. Honjo, R. A. Krishfield, and J. Yang, Woods Hole Oceanographic Institution, Woods Hole, MA 02543, USA.